



Article

Understanding the Correlation between Landscape Pattern and Vertical Urban Volume by Time-Series Remote Sensing Data: A Case Study of Melbourne

Mengyu Ge ¹, Shenghui Fang ^{1,*}, Yan Gong ¹, Pengjie Tao ¹ , Guang Yang ² and Wenbing Gong ¹ 

¹ School of Remote Sensing Information Engineering, Wuhan University, Wuhan 430079, China; 2011302590205@whu.edu.cn (M.G.); gongyan@whu.edu.cn (Y.G.); pjtao@whu.edu.cn (P.T.); gongheng@whu.edu.cn (W.G.)

² School of Geography, South China Normal University, Guangzhou 510631, China; gyang@m.scnu.edu.cn

* Correspondence: shfang@whu.edu.cn; Tel.: +86-27-6877-1238

Abstract: Urbanization is changing the world's surface pattern more and more drastically, which brings many social and ecological problems. Quantifying the changes in the landscape pattern and 3D structure of the city is important to understand these issues. This research study used Melbourne, a compact city, as a case study, and focused on landscape patterns and vertical urban volume (volume mean (VM), volume standard deviation (VSD)) and investigate the correlation between them from the scope of different scales and functions by Remote Sensing (RS) and Geographic Information System (GIS) techniques. We found: (1) From 2000 to 2012, the landscape pattern had a trend of decreasing fragmentation and increasing patch aggregation. The growth of VM and VSD was more severe than that of landscape metrics, and presented a “high–low” situation from the city center to the surroundings, maintaining the structure of “large east and small west”. (2) Landscape pattern was found closely associated with the urban volume. In the entire study area, landscape pattern patches with low fragmentation and high aggregation were directly proportional to VM with high value, which represented high urbanization, and patches with high connectivity and fragmentation had a positive relationship with high VSD, which represented strong spatial recognition. (3) The urban volumes of different urban functional areas were affected by different landscape patterns, and the analysis based on the local development situation can explain the internal mechanism of the interaction between the landscape pattern and the urban volume.

Keywords: urbanization; remote sensing; landscape pattern; vertical urban volume; Melbourne



Citation: Ge, M.; Fang, S.; Gong, Y.; Tao, P.; Yang, G.; Gong, W. Understanding the Correlation between Landscape Pattern and Vertical Urban Volume by Time-Series Remote Sensing Data: A Case Study of Melbourne. *ISPRS Int. J. Geo-Inf.* **2021**, *10*, 14. <https://doi.org/10.3390/ijgi10010014>

Received: 28 November 2020

Accepted: 31 December 2020

Published: 5 January 2021

Publisher's Note: MDPI stays neutral with regard to jurisdictional claims in published maps and institutional affiliations.



Copyright: © 2021 by the authors. Licensee MDPI, Basel, Switzerland. This article is an open access article distributed under the terms and conditions of the Creative Commons Attribution (CC BY) license (<https://creativecommons.org/licenses/by/4.0/>).

1. Introduction

Urban expansion refers to a form of natural land conversion into buildings, impervious surfaces, and related foundation facility that occurs with population growth, product development, scientific progress, and industrial structure adjustment [1]. In the past few decades, with the rapid growth of the urban population and intensive human activities, many cities have experienced dramatic expansion [2–4]. More and more countries and regions believe that although the rapid urbanization process is of great significance in driving regional economic development and improving industrial structure, it is undeniable that it is destroying the natural environment and bringing about a series of problems, such as extreme climate [5], cultivated land loss [6], greenhouse effect [7], water-quality degradation [8], unbalanced green resources [9], etc. In some areas, the phenomenon of “ghost towns” has even occurred due to overexploitation and demographic imbalance [10]. Based on the current population growth rate and economic development level, urban expansion will likely continue.

Urban expansion resulted in the change of the original landscape pattern [11], which referred to the spatial structure characteristics of the landscapes that are geospatial units

composed of different kinds of ecosystem mosaics [12,13]. Detecting changes in the landscape pattern index through remote sensing can reflect the characteristics of urban expansion [14–16]. Effat used Landsat data to calculate the landscape index Shannon's Diversity Index (SHDI), supplemented by other data to detect and quantify the spatial pattern of Cairo [4]. Wei Ji. investigated urban sprawl from different scales through landscape indicators and found that the development characteristics of Kansas City [17]. Bosch explored the spatiotemporal patterns in the Swiss urban agglomerations at two characteristic spatial extents by landscape indicators and growth modes [18]. The analysis of the urban landscape pattern and its spatiotemporal change is an effective means to qualitatively reveal the characteristics of urban spatial structure changes.

In addition, there were also a large number of studies that used mathematical models to quantitatively analyze the relationship between landscape patterns and urbanization metrics. As the main body of a city, the spatiotemporal changes of buildings can reflect the expansion process of a city. The method of establishing a mathematical model with landscape metrics and 2D urbanization metrics to find the correlation between landscape pattern and the level of urbanization has been widely used. Qiu took Beijing as an example to study the relationship between the fragmentation degree of urban landscape and urbanization (PLANDU) and socioeconomic indicators [19]. Felt employed the National Land Cover Database Percent Developed Imperviousness dataset (PDI) that measured the percentage of impervious cover which indicated the development level to investigate the urban fragmentation patterns of small and mid-sized cities in Idaho, USA [20]. Patrik Silva used the built-up area to represent the degree of urbanization, revealing the driving mechanism of other socioeconomic factors on urbanization [21].

The literature described above has contributed to the quantification of the relationship between urban expansion and landscape pattern. However, most of the studies were based on a 2D plane to reflect the intensity of urban expansion. Since the beginning of the 21st century, compared with 2D plane expansion, the trend of vertical expansion is becoming more and more obvious. For compact cities with dense populations, limited expansion space, and tight land resources, 2D urban expansion indicators that ignore high-level information may not be enough to reflect the degree of urbanization. For example, shanty towns and commercial areas may have the approximate PLANDU but their urbanization degree was different. A few studies have specifically discussed the vertical expansion phenomenon. Based on GIS and high-resolution remote sensing images, Qin selected the weighted average height of buildings, the volume of buildings, 3D expansion intensity, and 3D fractal dimension to evaluate the 3D urban expansion of Yangzhou, China from 2003 to 2012, and found that Yangzhou experienced drastic changes in both the plane and the vertical direction [22]. He extracted architectural contours and height information of five periods and proved that vertical expansion was the dominant factor of valley city development [23]. Zhong studied the 2D urban landscape and 3D height of residential areas in Beijing in the past 60 years and proposed that it is necessary to consider the vertical dimension in the spatial pattern analysis [24]. Therefore, in these compact cities, it is more objective to express the degree of urban development by 3D metrics [25], such as building height and building volume [26], than 2D metrics. Also, it is more scientific to establish a quantitative model between landscape pattern and 3D metrics than to qualitatively express landscape responses of urban expansion or to establish a model between landscape pattern and 2D metrics. Furthermore, it is of great significance to study the relationship between landscape pattern and 3D urban volume, that is, the degree of urban development can be quickly and scientifically expressed by employing landscape pattern when the urban volume is hard to calculate.

This research selected two 3D urban volume metrics to characterize the degree of urbanization and the degree of urban differentiation in the vertical direction of Melbourne with the support of RS and GIS. We analyzed the changes in landscape pattern and 3D urban building volume from 2000 to 2012, and investigated the relationship between them in the entire study area and three typical urban functional areas, and put forward

corresponding development suggestions. This research was beneficial to an in-depth understanding of the relationship between urban landscape and urban volume in the process of urban expansion. The purposes of this study were as follows: 1. Explore the spatial-temporal changes of 2D landscape patterns and 3D urban volume in Melbourne since the 20th century; 2. Reveal the relationship between the landscape metrics and the urban volume in the entire area and different typical urban functional areas; 3. Based on the above internal connections, provide corresponding development suggestions for the future urban expansion of Melbourne.

2. Data and Methods

2.1. Study Area

Melbourne, the capital of Victoria, is the cultural and industrial center of Australia and has been rated as “most suitable for human habitation” by the Economist Intelligence Unit for several years. Melbourne is the second-most densely populated city in Australia and has a temperate maritime climate [27]. Spring lasts from September to November, followed by three other seasons [28]. The beautiful urban scenery and highly developed urban structures are integrated, which provides a reference for the development of other cities. In 2001, the population of Melbourne reached 3.5 million, and the strategic population analysis showed that the population may increase to 4.5 million in 2021 [29]. The massive increase in population led to urban problems such as air pollution and untimely public services have emerged. In 2002, the Victorian government launched the “Melbourne 2030” plan to alleviate such problems, aiming to build Melbourne into a “more compact” city and build a livable, prosperous, and sustainable city [30]. The main method was to strengthen the compactness of internal buildings and increase medium and high-density housing in limited space and to curb urban expansion, extend urban growth to the vertical direction, and improve land use efficiency. For Melbourne, the urbanization expressed by the 3D urbanization metrics is more convincing than the 2D urbanization metrics.

The research area of this paper was mainly located in the urban area of Melbourne about 230 km², including Melbourne CBD, East Melbourne, West Melbourne, North Melbourne, Parkville, Carlton, South Yarra, St. Kilda Road, Southbank, Docklands, some suburbs, and part of the waters of Phillip port. Figure 1 showed the location of the study area in Melbourne. The reasons for choosing this rectangular area were as follows: 1. The area included the city of Melbourne, which was highly urbanized, with dense urban buildings and intense human activities. 2. It was mentioned in Section 2.3 that the moving window analysis used in this study only evaluated the elements containing the whole (square) window, and the boundary effect was inevitable, so the selection of the square area can effectively avoid the influence of the boundary effect. 3. The DSM data used in this study was only slightly larger than the rectangular area of this study. For the convenience of the experiment, we chose the study area similar to the size of the DSM data.

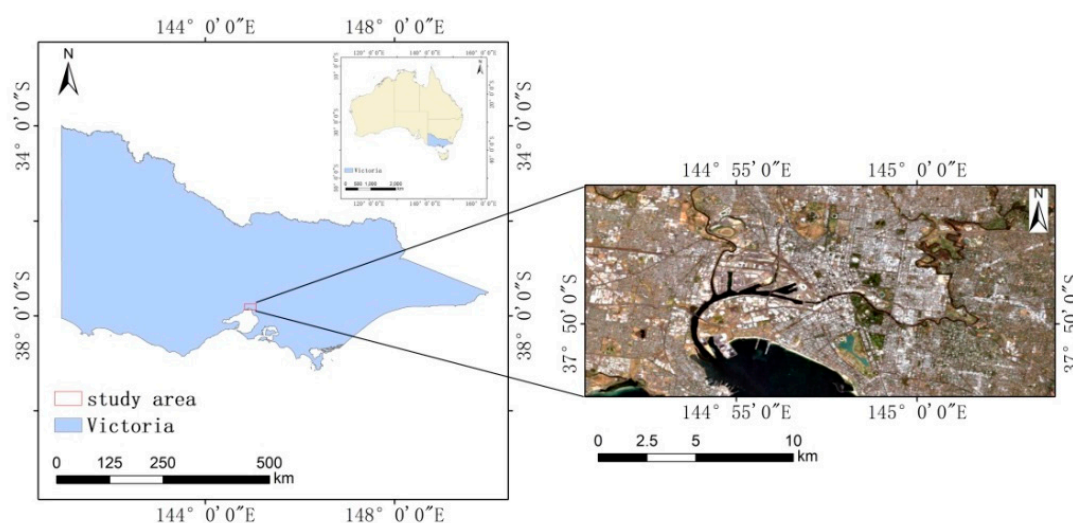


Figure 1. Location of the study area in Melbourne.

2.2. Workflow

As shown in Figure 2, the overall workflow was composed of three steps, landscape pattern calculation, urban volume calculation, and interaction analysis. Two datasets (Landsat images, Google Earth images) were used in the first step. The land use results in different years were generated by the Support Vector Machine (SVM) method and further used to derive landscape results based on eight landscape metrics in four aspects. In the second step, after preprocessing, elevation datum conversion, and manmade coverage ROI interception, three types of elevation data (SRTM, DSM, and JZM) could be adopted to calculate the urban volume. Finally, we conducted correlation analysis in the entire study area and three typical urban functional areas to explore the interaction characteristics between landscape pattern and urban volume.

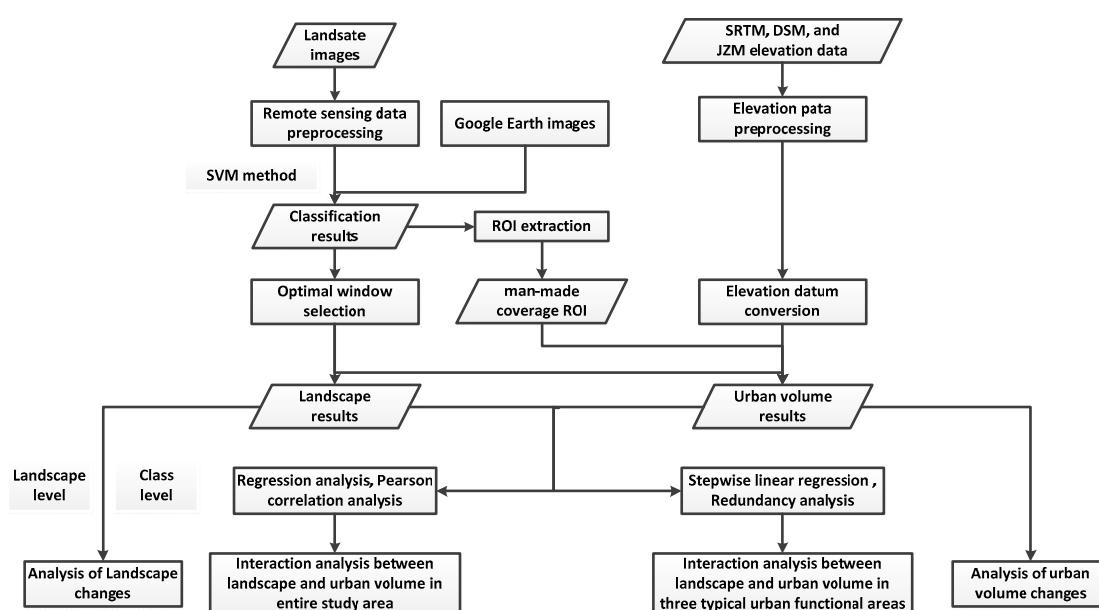


Figure 2. The flowchart of this study.

2.3. Remote Sensing Data Processing and Landscape Pattern Calculation

We chose Landsat images in 2000/2004/2008/2012 that were obtained from the USGS and had atmospherically corrected and geo-rectified. The spatial resolution was 30 m. According to the quality and availability of the data (cloud coverage rate was less than 1%), and considering that the seasonal change of land use in Melbourne is small [31], we selected Landsat7 data in 2000 and 2012, Landsat5 data in 2004 and 2008. Bands appeared in the Landsat7 data in 2012, so we selected the Landsat5 data with no bands in the adjacent months of 2011 for filling. After radiometric calibration and FLAASH atmospheric correction, we obtained the data that could be classified and calculated.

Based on the results of previous studies and the characteristics of ground features in Melbourne [31], five land use types were defined (Table 1), including manmade coverage, waterbody, woodland, grassland, and bare land, which were basically consistent with international classifications, such as CORINE land-cover (CLC) data, although this data set only provided information for a substantial part of Europe, rather than Australia [32]. For instance, manmade coverage, in our study area, contained residential construction, public facilities, transportation facilities, and other construction lands, etc., which was similar to artificial surfaces defined as Level 1 in CORINE land-cover nomenclature, that contained urban fabric, industrial, commercial and transport units, mine, dump and construction sites, and artificial nonagricultural vegetated areas. Waterbody referred to the part of the Pacific Ocean, Yarra River, and some ponds. Woodland contained natural reserves in the city, which included different kinds of broad-leaved forests, coniferous forests, and mixed forests. Different from natural grassland in CORINE land-cover nomenclature, grassland in our study mainly referred to artificial green spaces including gardens, and football fields. Bare land was the surface with no vegetation that was similar to the definition in CORINE land-cover nomenclature [33].

Table 1. Interpretation of land types and landscape category number.

Land Use Types	No.	Feature Types Included in Melbourne	Corresponding Types in CORINE Land-Cover Nomenclature
Manmade coverage	1	Residential construction, public facilities, transportation facilities, and other construction lands, etc.	Artificial surfaces
Waterbody	2	Ocean, urban rivers, ponds, etc.	Water bodies
Woodland	3	Street trees and natural reserves, etc.	Forest
Grassland	4	Gardens, football fields, etc.	No
Bare land	5	The land where the surface is soil and is not covered by vegetation	Open spaces with little or no vegetation

We combined high-resolution images in Google Earth to collect samples [34,35] and adopted the Support Vector Machine (SVM) classifier for classification [33,36]. The overall accuracy (OA) of the classification results were greater than 90%, and the results passed the Kappa coefficient test. The above steps were all carried out with the support of ENVI 5.3.

Landscape metrics highly condense landscape pattern information and are quantitative indicators that can reflect the composition of landscape structure and spatial configuration characteristics [37,38]. In our study, based on conceptual category, eight landscape metrics frequently used in the literature were selected for research in the four aspects of fragmentation, complexity, aggregation, and diversity. The explanation of the landscape metrics was shown in Table 2. For the class-level landscape metrics, we used the suffix according to the number in Table 1 to distinguish different land use types. For example, the proportion of manmade coverage was represented as “PLAND1”, the patch density of waterbody was represented as “PD2”, and so on.

Table 2. Metrics proposed to describe the urban landscape pattern.

Aspects	Landscape Metrics	Application Levels	Description
Fragmentation	Percentage of Landscape (PLAND)	Class	PLAND is the proportion of the area of the corresponding patch type in the total landscape area. In other words, PLAND is the proportional abundance of each patch type in the landscape, which provides basic information on the land use gradient [39].
	Patch Density (PD)	Class/Landscape	PD is the number of patches per unit area. Higher PD values indicate the increased extent of subdivision or fragmentation of the corresponding patch type [40].
	Largest Patch Index (LPI)	Class/Landscape	LPI is the percent of the total landscape area occupied by the largest size patch of the class of interest. The larger the LPI, the greater the impact of the largest patch on the whole landscape, and the higher the dominance of this type of patch [41].
Complexity	Landscape Shape Index (LSI)	Class/Landscape	LSI is calculated by the square amended total patch edge length divided by the total landscape area. LSI describes the complexity of the patch shape and the shape characteristics and possible evolutionary trends of the landscape spatial structure [42]. It is the most effective measure of overall shape complexity [43].
Aggregation	Aggregation Index (AI)	Class/Landscape	AI is the level of aggregation of spatial patterns. It means the non-randomness or aggregation degree of different patch types in the landscape [44].
	Contagion Index (CONTAG)	Landscape	CONTAG indicates the degree of reunion or extension of different patch types in the landscape. The probability of adjacent patches belonged to a class is calculated by the number of patches [42].
	Patch Cohesion Index (COHESION)	Class/Landscape	COHESION reflects the physical connectedness of the corresponding patch type and the continuity characteristics of each type. The larger the value, the stronger the continuity [45].
Diversity	Shannon's Diversity Index (SHDI)	Landscape	SHDI is based on Shannon's information-theoretic concept of entropy and is a measure of the degree of homogeneity and complexity of landscape types. The higher the SHDI is, the more abundant the land types are and the more uncertain the information content is. Diversity in landscape pattern is closely related to species diversity in ecology [46].

Moving window analysis can be used to quantify the landscape pattern in a specific range [46,47], clearly show the spatial realization process of the dynamic change of the urban landscape pattern. The landscape metrics are sensitive to spatial scale. Landscape heterogeneity is highly scale-dependent. If the window size is too large, the details will be lost, while if the window size is too small, the curve fluctuates too frequently, which is not conducive to analysis [48–50]. We conducted a series of extent analyses along the east–west direction of Melbourne City Hall, which was highly representative. Given the actual size of the study area, we chose 180 m, 360 m, 540 m, 900 m, 1200 m, 1500 m as the size of the moving window to achieve the spatial distribution map of the landscape-level metrics. As was shown in Figure 3, a smaller window size (less than 900 m) resulted in great fluctuations in the values of landscape metrics, while the curves were generally stable and the fluctuation ranges were close at larger window size (more than 900 m), so 900 m was the optimal scale of the moving window. Similar to the derivation of moving averages for a time series, this procedure smoothed out much of the noise caused by fine-scale and local variations [51].

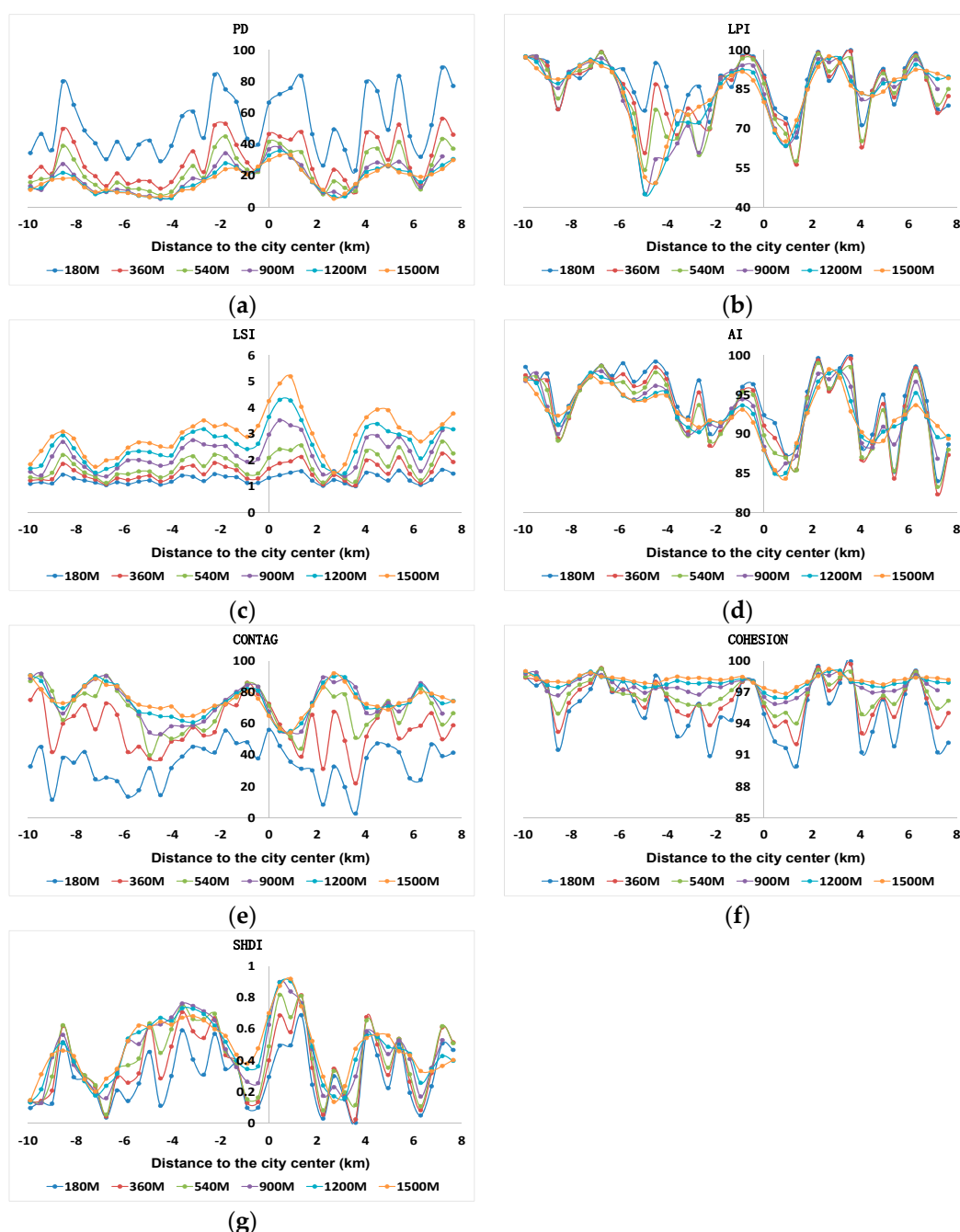


Figure 3. Curves of landscape metrics under different window sizes: (a) PD; (b) LPI; (c) LSI; (d) AI; (e) CONTAG; (f) COHESION; (g) SHDI. (Note: PD = Patch Density, LPI = Largest Patch Index, LSI = Landscape Shape Index, AI = Aggregation Index, CONTAG = Contagion Index, COHESION = Patch Cohesion Index, SHDI = Shannon's Diversity Index).

2.4. Elevation Data Processing and Volume Calculation

Shuttle Radar Topography Mission (SRTM) was carried out between the 11th and 20th of February 2000, onboard the space shuttle, 'Endeavour' [52]. SRTM began to be publicly released in 2003. After several revisions, the SRTM data used in this study was the 30-meter resolution V4.1 version obtained from the USGS. Compared with Digital Elevation Model (DEM) data, Digital Surface Models (DSM) data includes the elevation of other features above the ground surface [53], such as buildings and vegetation. The DSM data used in our study had a resolution of 1 meter, which was obtained after the dense matching of the stereo pair data of the French Pleiades-1A satellite in February 2012 [54]. Neither SRTM nor DSM

data showed data holes or abnormal shapes. The data of the bare-earth height information ('JZM' by default) used in this study was based on the observation of new-generation earth observation satellite TERRA. Existing studies have shown that the terrain feature lines extracted based on Google Earth elevation are consistent with the Google Earth image, and the accuracy is better than 1:50,000 topographic maps [55]. The spatial resolution of Google Earth elevation data extracted in this study area was approximately 15 m.

Many studies have defaulted that SRTM is a kind of DEM data [56,57]. However, it is often overlooked that SRTM is DSM, not DEM because SRTM includes the height of dense canopy forests and built-up areas [58–60]. The study area contained a large number of buildings and woodland, so SRTM and DSM contained the height of buildings in 2000 and 2012, respectively. The differences between SRTM, DSM, and JZM data were shown in Figure 4. This area was located in the center of Melbourne and contained a lot of buildings and a small number of forests. The mean elevation values of SRTM, DSM, and JZM in this area were 35.23 m, 37.23 m, and 25.47 m, respectively. In the same elevation data, the brighter place had the higher the elevation, and the darker place had the lower the elevation. We could see the distribution of buildings from the obvious spatial differences within SRTM and DSM. JZM reflected the elevation of the ground and the image was smooth, it was difficult to see the characteristics of buildings.

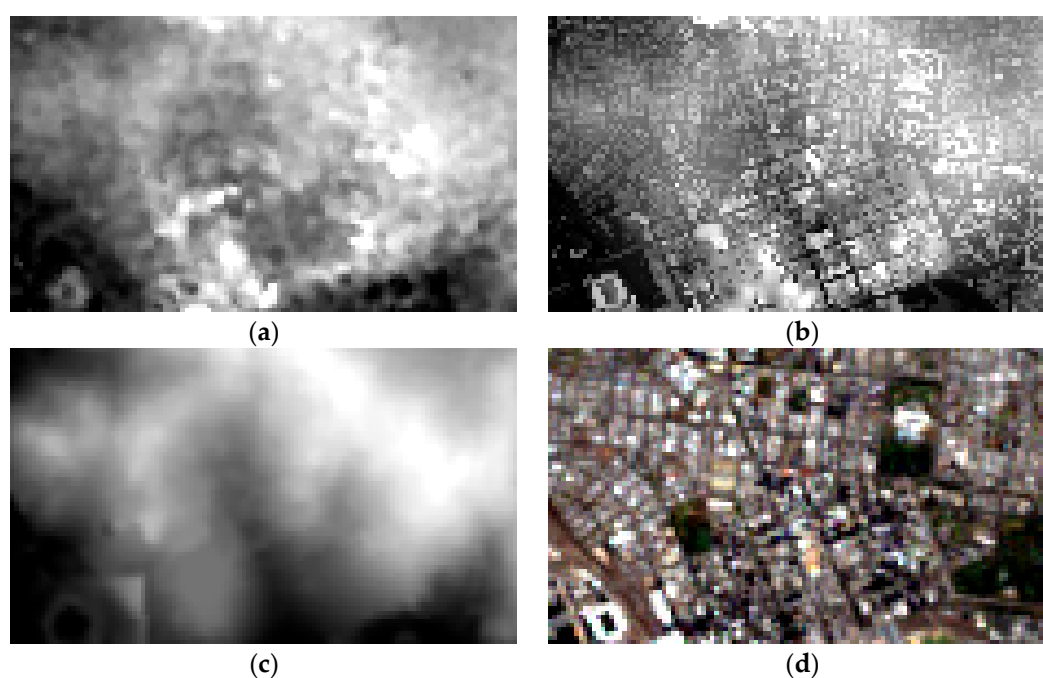


Figure 4. Different types of elevation data in Melbourne city center: (a) SRTM; (b) DSM; (c) JZM; (d) 2012 Landsat image.

We converted map projections of the three pieces of elevation data that had been resampled to a resolution of 30 meters to UTM with the nearest neighbor method for integration with classification results. Besides, the SRTM elevation datum was the normal height, corresponding to the quasi-geoid, the DSM elevation datum was the geodetic height, corresponding to the reference ellipsoid, and the JZM elevation datum was the orthometric height, corresponding to the geoid. The study area was small and located in the coastal plain area, which meant that the quasi-geoid and the geoid overlapped [61]. Only the height anomaly between the reference ellipsoid and the quasi-geoid needed to be solved. Molodensky, Bursa, and 4-parameter estimation algorithms, etc., have been widely used in practice [62–64]. Our study was limited by no GPS control points and local gravity data, and the terrain in the study area had small undulations, the grid coordinate transformation method based on the least square regression method was adopted. With the aid of Landsat imagery in 2000 and 2012 and the historical Google Earth imageries, we

selected 100 public points with no change that uniformly distributed within the research area through visual interpretation and recorded the value of 100 points in DSM and SRTM and calibrate the elevation datum of DSM and SRTM by the linear model. The correction formula was:

$$\text{DSM}' = (\text{DSM} - 1.884) \div \text{SM} - 1.88R^2 = 0.99, P < 0.01 \quad (1)$$

Among them, DSM' was the converted elevation data, and DSM was the original elevation data.

Previous studies often obtained building height directly from government departments [65] or airborne Lidar systems [66] or obtained the specific number of floors of building from real estate websites (e.g., Lianjia, Anjuke) and street view maps (e.g., Baidu Street View), and then multiplied the fixed floor height (e.g., 3m) to get the height of the building [24]. This study did not focus on the height of specific buildings but the continuous elevation of the study area.

The volume is equal to the area multiplied by the elevation, so on the premise of the same area (30 m \times 30 m), the elevation of manmade coverage is introduced to calculate the urban volume in the study area. Firstly, we subtracted JZM from SRTM and DSM to obtain the elevations of all features above the surface in 2000 and 2012. Secondly, we used the manmade coverage ROI in 2000 and 2012 to intercept the elevation data in 2000 and 2012, respectively. The elevation of all non-manmade coverage areas had defaulted to 0. Finally, we regarded the volume of Melbourne city as a spatial polyhedron composed of cuboids with the same base area and different heights (manmade coverage elevations), which was equal to the sum of cuboid accumulations, and the volume of each cuboid was the volume corresponding to each manmade coverage pixel. The urban volume in this study was continuous and included not only buildings but also other manmade coverage categories, such as viaducts, roads, which could fully reflect the changing trend of all manmade coverage volume. We chose volume mean (VM) and Volume Standard Deviation (VSD), which were representative to measure the changes in urban volume [67,68].

VM was used to express the amount of artificial coverage volume in the area. Generally speaking, the higher the VM of the area, the larger the volume of manmade coverage in the area, and the higher level of urbanization [25]. The calculation formula was:

$$\text{VM}_j = \frac{\sum_{i=1}^m V_i}{m} \quad (2)$$

VM_j , m , V_i were respectively the mean value of the urban volume, the total number of pixels, and the volume of the i th pixel (if it was not manmade coverage, the volume was 0) in the j th area.

The urban form was the core element of urban sustainability [14]. VSD was an important form feature of the vertical space development of modern cities and one of the important contents of urban landscape shaping [68]. We used VSD to reflect the degree of deviation of the volume in a certain area. The intensity of land development in different urban areas was different in sensitivity to land prices and market resource allocation and directly leads to the differential development of land development capacity and urban volume [69,70]. The larger the VSD, the more differentiated the vertical direction of the city, and the stronger spatial recognition, which helped to shape a more iconic and recognizable city intention and guide the block to make full use of its advantages to forming a more differentiated and intensive development model. The calculation formula was:

$$\text{VSD}_j = \sqrt{\frac{\sum_{i=1}^m (V_i - \text{VM}_j)^2}{m}} \quad (3)$$

VSD_j , m , V_i , and VM_j were respectively the standard deviation of the urban volume, the total number of pixels, and the volume of the i th pixel (if it was not manmade coverage, the volume was 0), and the mean value of the urban volume in the j th area.

2.5. Statistical Analysis

Regression analysis, Pearson correlation analysis, stepwise linear regression (SLR), and Redundancy Analysis (RDA) were applied to explore the relationship between urban landscape metrics and 3D urban volume.

We used regression analysis and Pearson correlation analysis to directly show the significant relationship between each landscape metric and urban volume metric from the perspective of the entire study area, as well as the degree of influence each landscape metric has on the urban volume. We applied frequently-used regression models such as linear, quadratic polynomial, logarithm, power function, exponential, etc., and then selected the model with the highest determination coefficient R^2 (Determining coefficient), and conducted significance tests ($p = 0.05$ or 0.01) to clarify the landscape factors that had a high correlation with the urban volume. The positive and negative correlations were determined through the Pearson correlation coefficient. This step was processed on SPSS 26.

For main functional areas (industrial area, commercial area, and residential area), SLR was used to select class-level landscape metrics that were sensitive to urban volume, and then RDA analysis was used to rank these factors. Firstly, we standardized the class-level landscape metrics (explanatory variable), and volume metrics (dependent variable) to eliminate the differences in dimensions in the SLR analysis [71]. The class-level landscape metrics with high collinearity were tested and deleted through the VIF (variance inflation factor, $VIF < 10$) and Tolerance (Tolerance > 0.1) to make sure that landscape metrics entered in the RDA analysis were independent [72,73]. Finally, we set the class-level landscape metrics selected by SLR analysis as environment variables and the volume metrics as species variables for RDA analysis. Based on the results of RDA, we discussed the inner relationship between the two most explanatory landscape factors and urban volume metrics [74–76]. As one form of asymmetric canonical analysis, RDA has been widely employed by ecologists and paleoecologists. SLR was processed on SPSS 26 and RDA was run on the CANOCO 5.0 program (Microcomputer Power Company, USA).

3. Results

3.1. The Spatiotemporal Pattern of Landscape and Volume

3.1.1. Landscape Pattern Changes

Figure 5 presented the land-cover maps of 2000, 2004, 2008, 2012. The transfer matrix of land use types from 2000 to 2012 was calculated. Table 3 showed that manmade coverage continued to expand and dominate, increasing by 23.03 km^2 , benefited from the conversion of woodland, grassland, and bare land. The area of grassland and bare land decreased sharply by 7.19 km^2 and 13.25 km^2 , respectively. In addition to manmade coverage, 4.51 km^2 of grassland was converted into woodland, and 1.44 km^2 and 2.78 km^2 of bare land were converted into woodland and grassland, respectively, which also resulted in the overall area of woodland unchanged, although 8.44 km^2 of woodland was converted to artificial coverage. The water body was relatively stable.

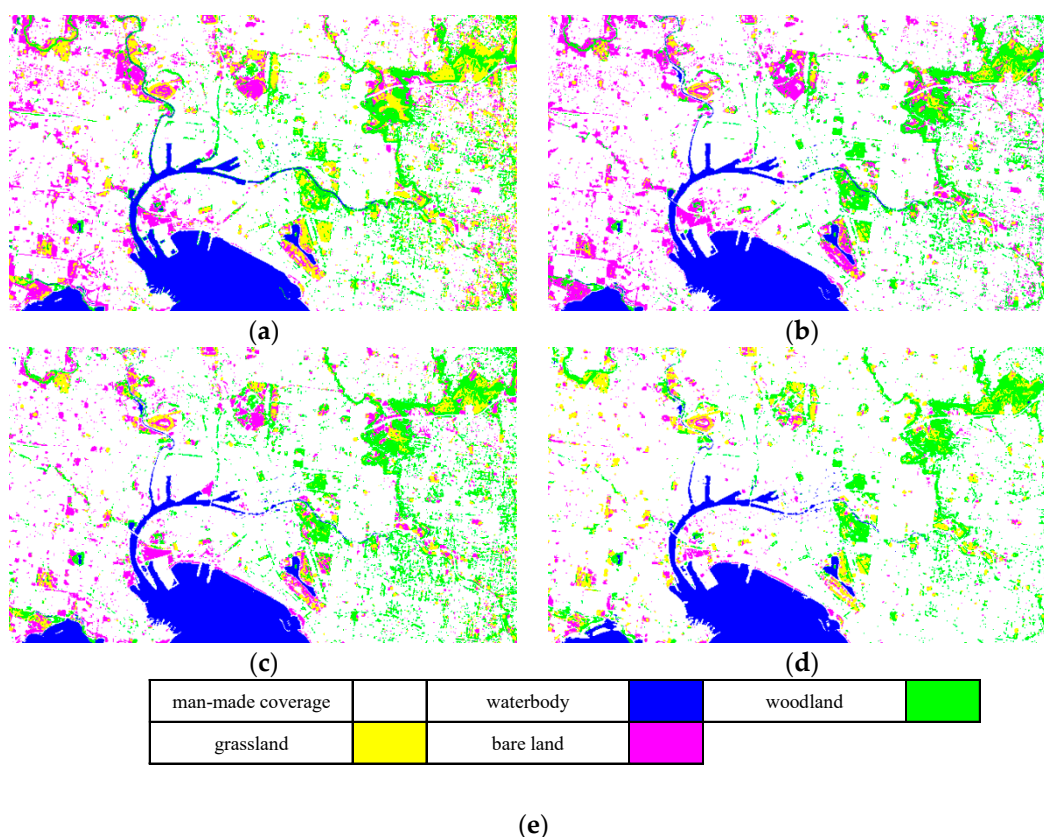


Figure 5. Classification maps of Melbourne from 2000–2012: (a) 2000; (b) 2004; (c) 2008; (d) 2012; (e) Legend of classification results.

Table 3. Transfer matrix of land use types from 2000 to 2012 (km²).

2012 \ 2000						
	Manmade Coverage	Waterbody	Woodland	Grassland	Bare Land	Total Area in 2000
manmade coverage	152.17	1.38	8.44	5.18	11.31	178.49
waterbody	0.17	17.01	0.11	0.01	0.04	17.35
woodland	1.20	0.10	8.91	4.51	1.44	16.16
grassland	0.46	0.00	0.09	7.09	2.78	10.42
bare land	1.45	0.01	0.03	0.82	2.77	5.09
total area in 2012	155.45	18.51	17.59	17.61	18.35	227.50
Area change	23.03	−1.16	−1.43	−7.19	−13.25	

For class-level landscape metrics, Table 4 showed that from 2000 to 2012, as the most important landscape type, manmade coverage had a similar change with woodland and grassland in the process of urbanization, that was, the degree of fragmentation and complexity decreased, the aggregation increased, and the patches became regular and reunite. The landscape metrics of bare land dropped sharply, and of the water were generally stable.

For landscape-level landscape metrics, to avoid data redundancy, we only selected PD, LSI, AI, and SHDI, which respectively represented fragmentation, complexity, aggregation, and diversity in the landscape-level metrics for discussion. Figure 6 showed a downward trend in PD, LSI, and SHDI, while AI increased. The main land use type in the study area was manmade coverage, it indicated that in the 2D plane, with the development of urbanization, the distribution was more close, the dominance was enhanced, and the influence was increased, which also brought about the degree of landscape-level heterogeneity and diversity reduction. Also, each index fluctuated in 2004 and 2008.

Table 4. Class-level metrics change from 2000 to 2012.

Land Use Types	Years	PLAND	PD	LPI	LSI	AI	COHESION
Manmade Coverage	2000	68.33	1.95	62.52	35.04	91.78	99.90
	2004	72.16	1.42	70.05	31.14	92.92	99.93
	2008	73.46	1.79	72.55	32.74	92.61	99.95
	2012	78.45	1.16	76.64	22.52	95.15	99.95
Waterbody	2000	8.13	0.49	6.99	7.74	95.27	98.81
	2004	8.14	0.46	6.94	7.99	95.09	98.80
	2008	7.93	0.57	6.14	7.94	95.05	98.20
	2012	7.62	0.69	6.07	7.86	95.01	98.16
Woodland	2000	7.73	11.84	2.02	61.91	56.05	92.43
	2004	7.91	9.69	1.13	54.16	62.10	91.81
	2008	8.76	11.84	1.03	62.06	58.65	89.95
	2012	7.10	7.89	1.30	47.63	64.93	92.28
Grassland	2000	7.74	9.29	0.36	50.05	64.64	84.50
	2004	2.72	3.13	0.12	31.19	63.15	84.24
	2008	4.03	7.44	0.28	44.77	56.19	81.44
	2012	4.58	3.85	0.15	35.23	67.76	85.47
Bare Land	2000	8.06	12.87	0.28	58.76	59.20	83.06
	2004	9.07	13.36	0.55	59.43	61.13	85.02
	2008	5.82	9.17	0.18	48.86	60.12	79.72
	2012	2.24	4.90	0.10	36.81	51.60	71.43

(Note: PLAND = Percentage of Landscape, PD = Patch Density, LPI = Largest Patch Index, LSI = Landscape Shape Index, AI = Aggregation Index, COHESION = Patch Cohesion Index).

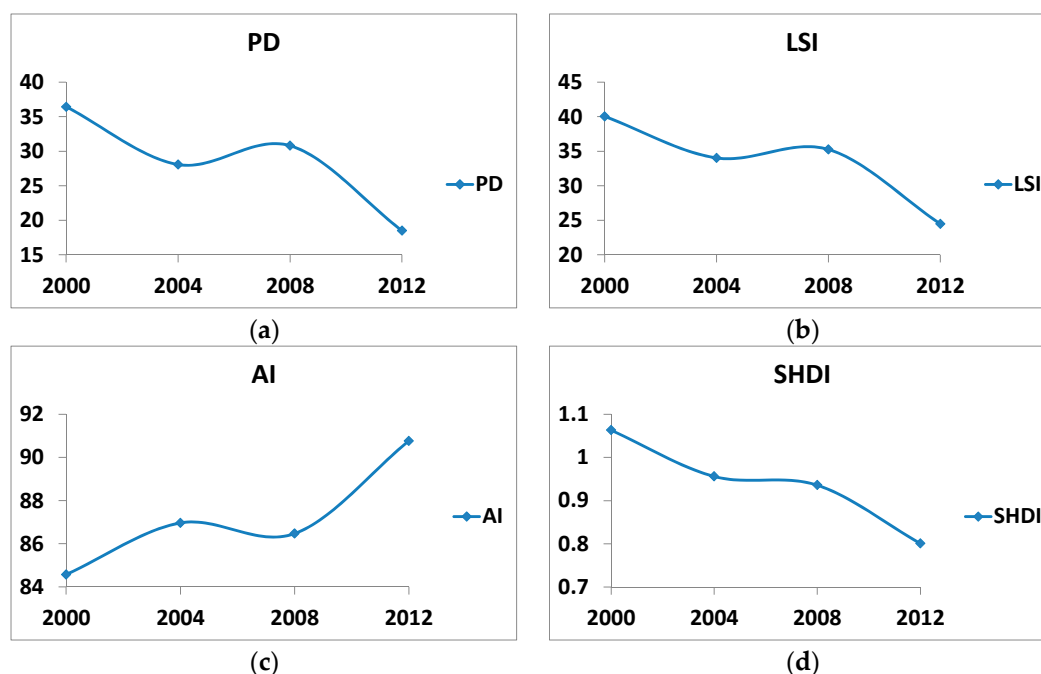


Figure 6. Landscape-level metrics change from 2000 to 2012: (a) PD; (b) LSI; (c) AI; (d) SHDI. (Note: PD = Patch Density, LSI = Landscape Shape Index, AI = Aggregation Index, SHDI = Shannon's Diversity Index).

3.1.2. Urban Volume Change

In order to intuitively reflect the overall urban volume changing trend of Melbourne and combine volume with the landscape metrics for analysis, the volume distribution maps were also calculated using a 900-meter moving window. VM per unit area of Melbourne

increased from 2942.28 m³ in 2000 to 4861.72 m³ in 2012, an increase of 65.24%, and an average annual growth rate of 5.44%. VSD increased 2474.99 m³ from to 3648.57 m³. Correspondingly, PLAND1 only increased from 68.33% to 78.45%, an increase of 10.12%, with an average annual growth rate of only 0.843% (Table 5).

Table 5. The changes of VM and VSD from 2000 to 2012 (m³).

	2000	2012	Volume Change	Change Rate
VM	2942.28	4861.72	1919.44	5.44%
VSD	2474.99	3648.57	1173.58	3.95%

(Note: VM = volume mean, VSD = Volume Standard Deviation).

Figures 7 and 8 showed that VM varied in space and formed a “high-low” pattern from the city center to the surrounding areas, and formed a “big east and small west” structure. The VM range to the west of the city center rose from 0 m³–2700 m³ to 2700 m³–5400 m³, and to the east of the city center rose from 2700 m³–5400 m³ to 5400 m³–8100 m³. The areas with VM higher than 8100 m³ were mainly located in the vicinity of the city center. Among them, the area of 8100 m³–10,800 m³ rose from 0.61% in 2000 to 1.82% in 2012, and the area higher than 10,800 m³ rose from 0.81% to 1.17%. In 2000, the area with VM less than 5400 m³ reached 95.41%, while in 2012 it only accounted for 58.47%. The area between 5400 m³–8100 m³ increased significantly, from 3.17% in 2000 to 38.54% in 2012.

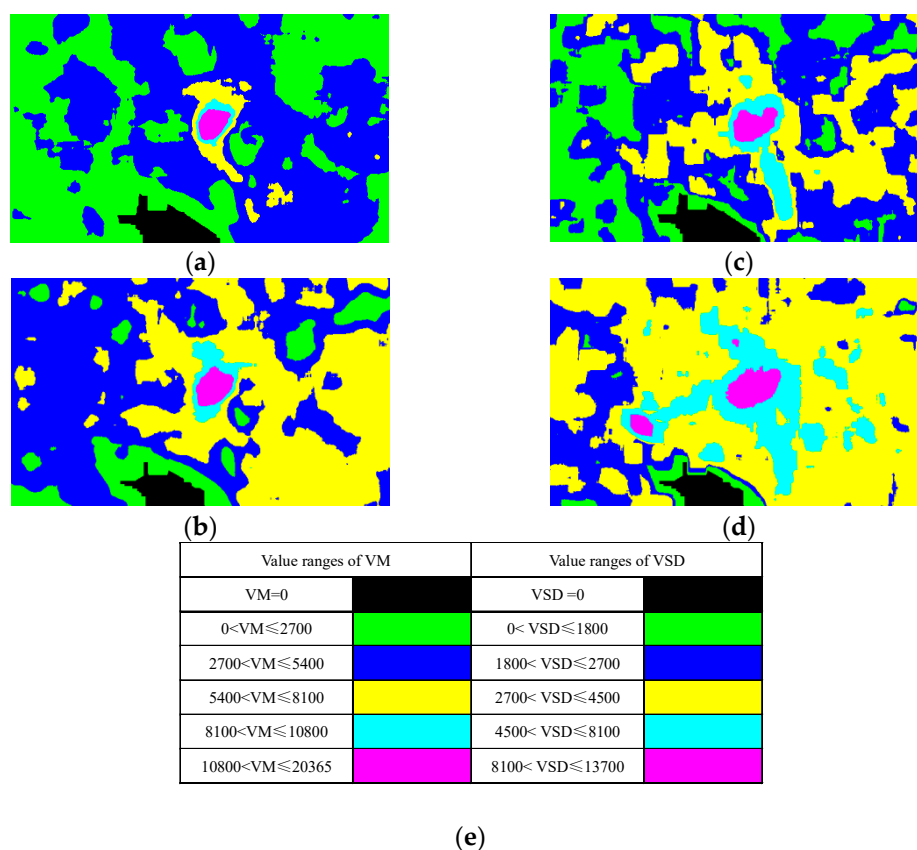


Figure 7. Distribution maps of VM and VSD in 2000 and 2012: (a) 2000 VM; (b) 2012 VM; (c) 2000 VSD; (d) 2012 VSD; (e) Value ranges of VM and VSD. (Note: VM = volume mean, VSD = Volume Standard Deviation).

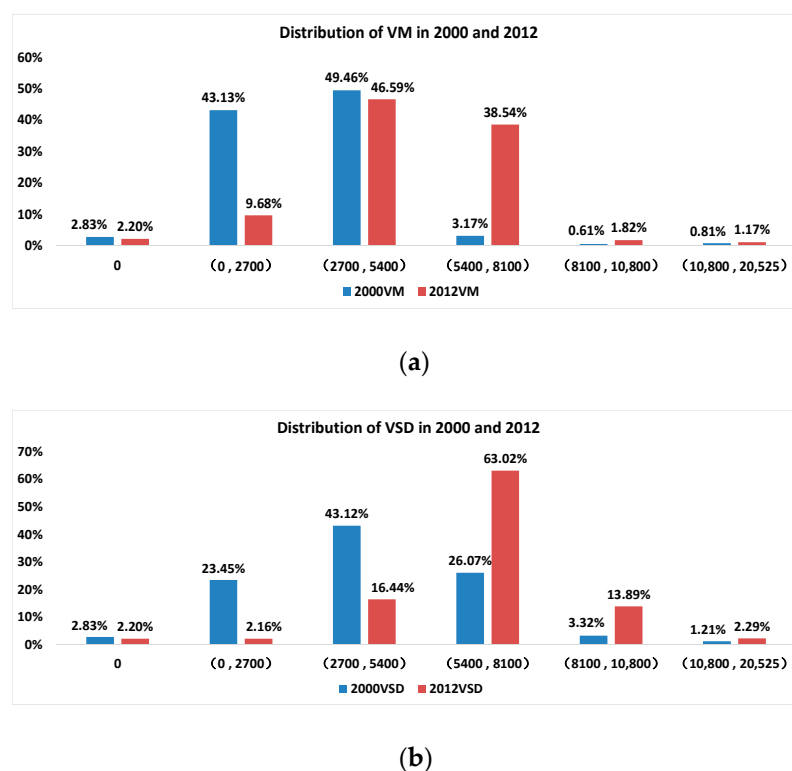


Figure 8. Interval distribution of VM and VSD in 2000 and 2012: (a) VM; (b) VSD. (Note: VM = volume mean, VSD = Volume Standard Deviation).

As was shown in Figure 7, VSD in the west of the city center was smaller than that in the east, mainly because the west was relatively underdeveloped, and the buildings were mainly low-rise buildings with less differentiation. The difference from VM was that in areas with VSD greater than 4500 m³, in addition to the east–west spread, the north–south spread was also obvious.

3.2. Correlation and Changes within Different Areas

3.2.1. Entire Study Area

Both VM and VSD had close relationships with landscape metrics.

In landscape-level metrics, VM and CONTAG ($R^2_{2000} = 0.30$, $R^2_{2012} = 0.48$) were closely related (Table A1), VSD was closely related to PD ($R^2_{2000} = 0.39$, $R^2_{2012} = 0.33$) and SHDI ($R^2_{2000} = 0.51$, $R^2_{2012} = 0.30$) (Table A2). According to the Pearson correlation coefficient, VM and CONTAG, VSD and PD, SHDI were all positively correlated.

In class-level metrics, Table A1 (Appendix A) showed that a high correlation appeared between VM and manmade coverage, waterbody, instead of woodland, grassland, and bare land. Where VM and PLAND1 ($R^2_{2000} = 0.88$, $R^2_{2012} = 0.92$), LPI1 ($R^2_{2000} = 0.85$, $R^2_{2012} = 0.91$), AI1 ($R^2_{2000} = 0.81$, $R^2_{2012} = 0.82$), COHESION1 ($R^2_{2000} = 0.87$, $R^2_{2012} = 0.88$), PLAND2 ($R^2_{2000} = 0.57$, $R^2_{2012} = 0.65$), LPI2 ($R^2_{2000} = 0.58$, $R^2_{2012} = 0.66$) were highly correlated. Except for the negative correlation between VM and PLAND2, LPI2, the correlation between VM and other metrics were all positive. Table A2 indicated that VSD was closely related to manmade coverage, waterbody, and woodland, and had no obvious correlation with grassland and bare land. VSD and PLAND1 ($R^2_{2000} = 0.57$, $R^2_{2012} = 0.55$), LPI1 ($R^2_{2000} = 0.50$, $R^2_{2012} = 0.51$), LSI1 ($R^2_{2000} = 0.46$, $R^2_{2012} = 0.39$), AI1 ($R^2_{2000} = 0.62$, $R^2_{2012} = 0.55$), COHESION1 ($R^2_{2000} = 0.70$, $R^2_{2012} = 0.63$), PLAND2 ($R^2_{2000} = 0.38$, $R^2_{2012} = 0.37$), PD2 ($R^2_{2012} = 0.37$), LPI2 ($R^2_{2000} = 0.40$, $R^2_{2012} = 0.40$), PD3 ($R^2_{2000} = 0.30$), LSI3 ($R^2_{2000} = 0.31$) were highly correlated. Except for the negative correlation with PLAND2 and LPI2, VSD was positively correlated with other metrics.

3.2.2. Three Typical Urban Functional Areas

The previous section reflected the relationship between the entire landscape pattern and the overall volume, but for different regions, we did not know whether the above landscape metrics and urban volume still maintained such a high correlation. In order to solve this problem, three main functional areas (industrial area, commercial area, and residential area) were analyzed.

The industrial area consisted of industrial plants and some residential buildings, near the junction of the Maribyrnong and Yarra River. In the industrial area, the landscape metrics with a high correlation of city volume in 2000 were LPI3, AI3, PD4, LPI4, LPI4, COHESION4, PD5, LPI5, AI5, and COHESION5, in 2012 were COHESION2, PLAND3, PD3, and PD4. There was a high relationship between water, woodland, grassland, bare land, and urban volume in the industrial area (Table A3).

The commercial area was distributed along both sides of Yarra River, consisting of the CBD and parts of the South Bank, with a high level of urbanization. The Yarra River straddled the downtown area of Melbourne. In the mid-nineteenth century, the development on both sides of the Yarra River was uneven, but after several renovations, the waterfront areas on both sides of the Yarra River had become commercial and cultural centers of Melbourne. The phenomenon of imbalance and fragmentation had disappeared, so this study also considered parts of the South Bank as the commercial area [77]. In the commercial area, the landscape metrics with high correlation of urban volume in 2000 were PD2, COHESION2, PD4, AI4, LSI5, and AI5, in 2012 were PD2, AI3, LSI4, LSI5, and AI5. There was a close relationship between water, woodland, grassland, bare land, and urban volume in the commercial area (Table A4).

The residential area was mainly located in Richmond. In the residential area, in 2000, the metrics with high correlation with the city volume were PD1, LPI1, PD3, COHESION3, PLAND4, AI4, COHESION4, and LSI5. In 2012, there were LSI3, COHESION3, PLAND4, AI4, LPI5, and LSI5. There was a high relationship between manmade coverage, woodland, grassland, bare land, and urban volume in the residential area (Table A5).

We used RDA analysis to quantify the contribution of key landscape metrics to urban volume. In the industrial area, the interpretation of landscape metrics to urban volume reached 76.6% in 2000, with PD5 having the highest degree of explanation (43.5%), and COHESION3 second (9.9%). PD5 was significantly positively correlated with VM and significantly negatively correlated with VSD, COHESION3 was negatively correlated with VM and positively correlated with VSD (Figure 9). In 2012, the interpretation of landscape metrics to urban volume reached to 50.9%. PD4 had the highest degree of explanation for urban volume (35.8%), followed by COHESION2 (11.3%). PD4 was positively correlated with VM, and negatively correlated with VSD, COHESION2 and VM showed a negative correlation and a positive correlation with VSD (Figure 9).

In the commercial area, landscape metrics accounted for 64.2% of the urban volume in 2000, with LSI5 having the highest degree of explanation (38.8%), and COHESION3 second (19.5%). LSI5 was negatively correlated with VM and VSD, and PD2 was positively correlated with VM and VSD (Figure 10). In 2012, landscape metrics accounted for 60.1% of the urban volume, of which LSI4 explained the urban volume the highest (29.1%), followed by PD2 (15.8%). Among them, LSI4 was negatively correlated with VM and VSD, and PD2 was positively correlated with VM and VSD (Figure 10).

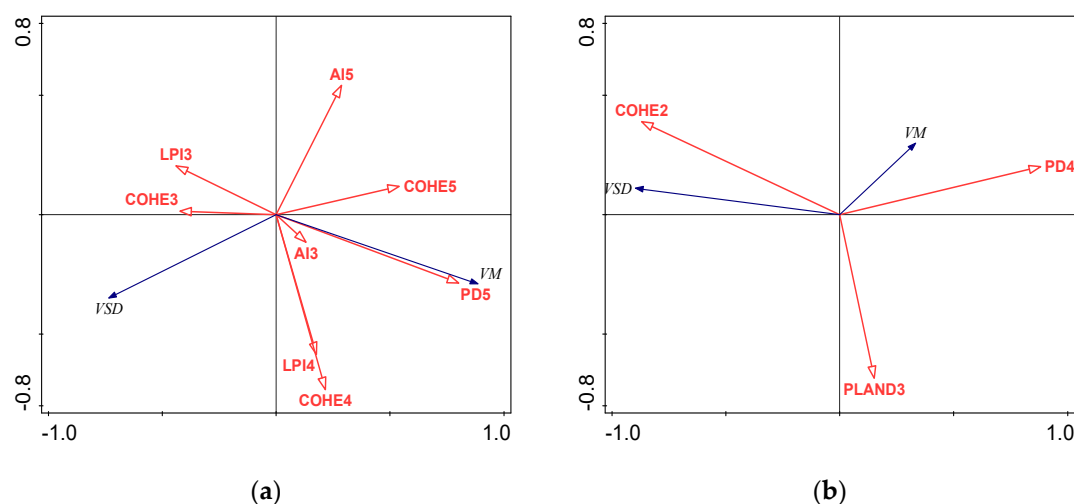


Figure 9. RDA ordination diagram with VM, VSD, and landscape metrics in the industrial area (COHESION was abbreviated as COHE due to length limitation): (a) 2000; (b) 2012. (Note: PLAND = Percentage of Landscape, PD = Patch Density, LPI = Largest Patch Index, LSI = Landscape Shape Index, AI = Aggregation Index, CONTAG = Contagion Index, COHESION = Patch Cohesion Index. VM = volume mean, VSD = Volume Standard Deviation. 1 = Manmade coverage, 2 = Waterbody, 3 = Woodland, 4 = Grassland, 5 = Bare land).

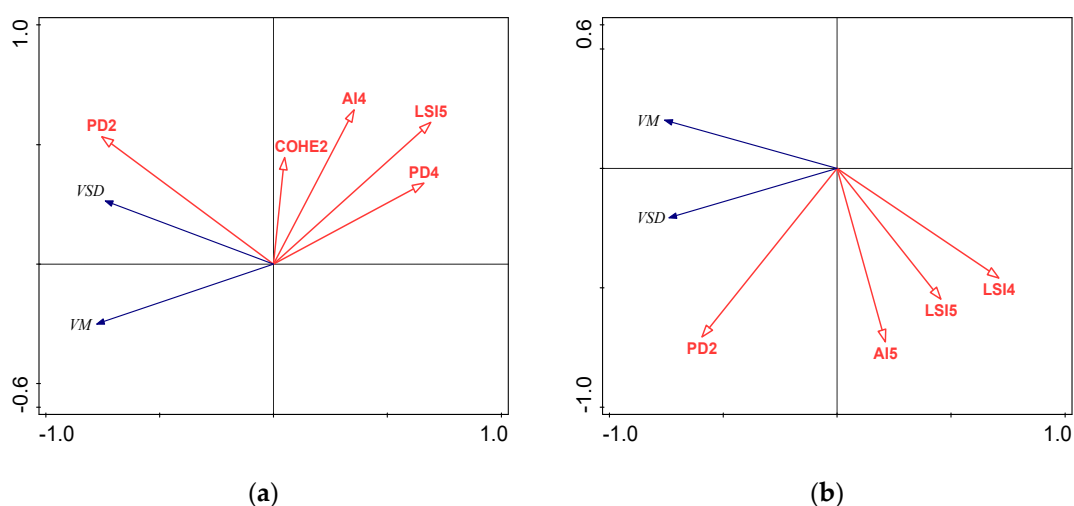


Figure 10. RDA ordination diagram with VM, VSD, and landscape metrics in the commercial area (COHESION was abbreviated as COHE due to length limitation): (a) 2000; (b) 2012. (Note: PLAND = Percentage of Landscape, PD = Patch Density, LPI = Largest Patch Index, LSI = Landscape Shape Index, AI = Aggregation Index, CONTAG = Contagion Index, COHESION = Patch Cohesion Index. VM = volume mean, VSD = Volume Standard Deviation. 1 = Manmade coverage, 2 = Waterbody, 3 = Woodland, 4 = Grassland, 5 = Bare land).

In the residential area, landscape metrics could explain 85.0% of the urban volume changes in 2000. Among them, LPI1 explained the urban volume the most (77.4%), and the other variables explained little (<2.7%) (Figure 11). In 2012, landscape metrics could explain 62.9% of urban volume changes, of which LSI3 had the highest degree of explanation for urban volume (31.5%), LPI5 and PLAND4 had similar explanations, 15.2%, and 14.3%, respectively, and the other variables had a fewer degree of explanation (<1.4%). Among them, LSI3 was negatively correlated with VM and positively correlated with VSD; LPI5 was positively correlated with VM and VSD; PLAND4 was negatively correlated with VM and VSD (Figure 11).

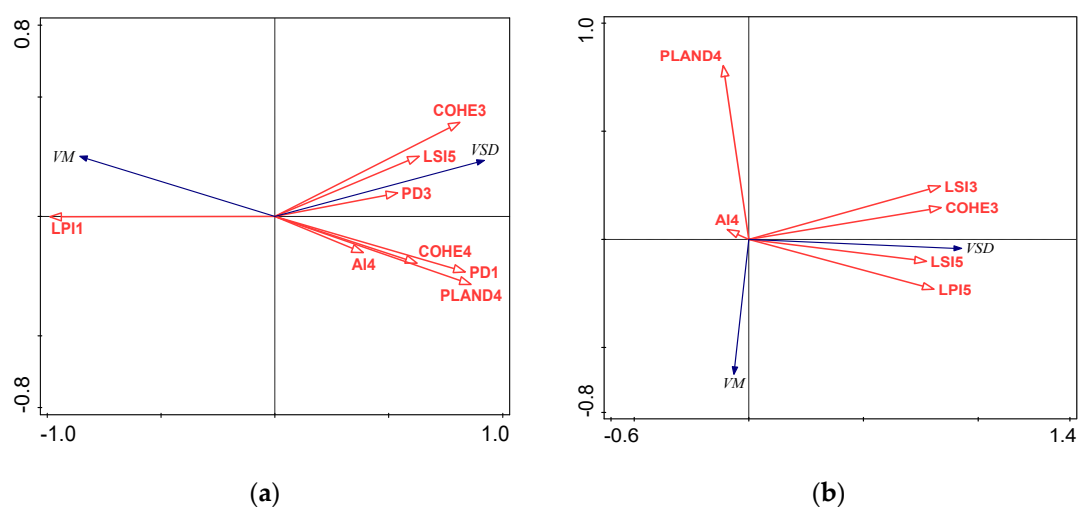


Figure 11. RDA ordination diagram with VM, VSD, and landscape metrics in the residential area (COHESION was abbreviated as COHE due to length limitation): (a) 2000; (b) 2012. (Note: PLAND = Percentage of Landscape, PD = Patch Density, LPI = Largest Patch Index, LSI = Landscape Shape Index, AI = Aggregation Index, CONTAG = Contagion Index, COHESION = Patch Cohesion Index. VM = volume mean, VSD = Volume Standard Deviation. 1 = Manmade coverage, 2 = Waterbody, 3 = Woodland, 4 = Grassland, 5 = Bare land).

4. Discussion

4.1. Reasons for the Change of Different Dimensions in Melbourne

Our study indicated that in the past 12 years, Melbourne had continuously evolved from a 2D development to a 3D development, and the development trend of the vertical direction of space had become more obvious and strong.

From 2000–2012, with the development of urbanization, manmade coverage was always the most important land use type, while a similar trend had appeared in woodland and grassland, that was, the degree of fragmentation and complexity decreased, and the connectivity increased. The patches became regular and reunite. All metrics of bare land dropped sharply, and water bodies were generally stable.

As the main landscape category, manmade coverage was in the stage of gradual aggregation, and regular shape. The internal connectivity was enhanced. The overall change of manmade coverage corresponded to the compact urban construction proposed in Melbourne 2030 [30]. The waterbody included part of the waters of Port Phillip Bay and the middle and lower reaches of the Yarra River. The government of Melbourne strictly protected water resources and had issued a series of policies, such as ensuring the sustainable management of water sources, protecting groundwater, and the bay area [78]. Only part of the water area was forced to fill up due to construction works, which caused a slight decrease in the water area. Woodland and grassland were belonged to green space and had the same change characteristics. Both of them gradually became gathered and less clumped. The woodland was mainly targeted at some natural reserves, while the grassland was mainly targeted at part of artificial green land, including gardens, and football fields. With the introduction of “Melbourne 2030” in 2002 [30], a large number of urban construction projects started, which led to a brief cliff-like decline in the grassland. But in order to meet the Commonwealth Games held in Melbourne in 2006, the government subsequently increased the area of urban green space and beautified the urban environment. The fragmentation and complexity of the grassland were reduced, and the grassland became less clumped. During this period, Melbourne had been rated as the “most suitable for human habitation” by the Population Action International for many consecutive years, earning Melbourne the “Garden City” reputation. In 2000, bare land was dominated by surface-shaped construction sites that appeared in urban construction. With the improvement of the internal environment of the city, the bare land subsequently

fell cliff-like. The decrease in bare land was accompanied by the increase in urbanization in Melbourne, reflecting the increase in the degree of intensification of urban land use.

In landscape-level metrics, PD, LSI, and SHDI decreased overall, and AI increased, which meant that the patch distribution became more concentrated, and the degree of landscape heterogeneity and diversity decreased. This was mainly due to the mature urban planning system and the implementation of sustainable development concepts in Melbourne.

Compared with the large-scale urban expansion in developing countries [79–81], since the beginning of the 21st century, the expansion of the urban area in Melbourne was not obvious. However, VM and VSD increased rapidly which indicated the pace of urbanization was accelerating and the differences in the vertical direction were great. Besides, both VM and VSD presented a “high–low” situation from the city center to the surroundings, maintaining the distribution of “large east and small west”, which may be due to unbalanced development level.

Our study demonstrated that the VM and VSD value increased overall, while PD and LSI, which represented 2D fragmentation and complexity, were generally reduced. This phenomenon showed that the development trend in the vertical direction of Melbourne was more intense.

4.2. Quantitative Analysis and Suggestions

4.2.1. Entire Study Area

Urban expansion is a dynamic phenomenon and is affected by many factors [82]. Our study indicated that in the entire study area, landscape pattern was found closely associated with urban volume, but different landscape metrics had a different correlation with volume metrics, which were affected by environmental characteristics, economic development level, and policy implementation.

Patches with low fragmentation and high aggregation were directly proportional to VM with high value. For example, in Hawthorn, 6 km east of the city center, driven by the metropolitan area development policies issued by the Victorian government such as “shaping Melbourne’s future”, “creating prosperity”, and “living in the suburbs”, population suburbanization and urban suburbanization were accelerating, and fringe cities were gradually formed. Low private houses rapidly spread, patches here were gradually developing in the direction of low fragmentation, low complexity, low diversity, and high connectivity, VM increased and the urbanization was subsequently strengthened.

Our study also indicated that different types of landscape metrics had the same correlation with VSD. VSD had a positive relationship with aggregation, such as AI1, COHESION1. For example, with the promotion of the “compact city” policy, more and more buildings had undergone reconstruction or expansion which resulted in high VM in CBD. Meanwhile, multi-story buildings, high-rise buildings, and super high-rise buildings were in contrast with other surrounding low buildings, leading to high VSD, and finally formed a spatial form with well-organized, distinct principal and subordinate, and strong recognition. However, VSD also had a positive relationship with fragmentation, diversity, and complexity. For example, Carlton was located 1.5 km north of the city center with high PD and SHDI. This area was a vibrant and diverse neighborhood with many museums (Melbourne Museum, Royal Exhibition Building), schools (Australian Catholic University), parks (Carlton Gardens, Quest Royal Garden), and large hospitals (St. Vincent’s Hospital). A complex patch meant a high land surface structure complexity [43]. The height differences between buildings and non-buildings (e.g., woodland areas) were relatively large. Therefore, the degree of differentiation in the vertical direction was improved. Furthermore, we could also found that the correlation between VSD and fragmentation was much less than that with connectivity. The reason may be that most of the study area was covered by buildings, and the probability of height differences between different buildings was much higher than that between buildings and non-buildings.

Our study also demonstrated an obvious negative relationship between both VM and VSD and waterbody landscape metrics. Melbourne thrived along the Yarra River where the highly fragmented water patches were mainly concentrated. There were dense and uneven buildings on both sides of the Yarra River, and part of the river was buried for construction and development in the process of urban expansion, which increased the degree of water fragmentation and reduced the superiority of the water body, increasing both urbanization and urban differentiation in the vertical direction nearby.

4.2.2. Three Typical Urban Functional Areas

Volume metrics in different areas had a different correlation with landscape metrics. To investigate the correlation in detail, we chose three typical urban functional areas to make a concrete and quantitative analysis.

Our study indicated that the urban volume metrics of the industrial area were highly correlated with the fragmentation of bare land and the aggregation of woodland in 2000, and were highly correlated with the fragmentation of grassland and the aggregation of the waterbody in 2012. In the industrial area, the renovation of the old factory buildings was being carried out in 2000 and bare land inevitably appeared. The high fragmentation of the bare land meant that the intensity of the renovation of the area was high, but due to the strong integrity of the architectural planning, the height differences of the factory buildings were relatively small. In the industrial area, the average VSD value was 2019.67 m^3 and the maximum VSD value was 2973.46 m^3 in 2000, both of them were much smaller than the average VSD of 2474.99 m^3 and the maximum value of $12,968.87 \text{ m}^3$ in the entire study area. Concentrated woodland took up more surface space, which meant that the VM in the area was reduced, but the differences between buildings and woodland would be more prominent, which brought about an increase in VSD. In 2012, both the renovation of the industrial area and the improvement of the environment were carried out. The industrial plants close to the Maribyrnong River and the Yarra River were partially demolished and replaced by patches of cement vacant land, resulting in a decrease in the original urban volume. But the industrial plants were tall and covered a large area, highlighting the improvement of VSD. Most of the grassland interspersed between residential houses. Compared with scattered industrial plants, VM here was relatively large, but the height differences were small. In the future, the government should not only implement standardized construction (such as overall demolition and reconstruction, reconstruction, and decoration without dismantling the mainframe structure) to attract more companies into the industrial zone but also make a scientific layout. Areas with higher fragmentation of green space around industrial plants should be emphasized. Also, factories should be organized to stay away from waterbody to protect the safety of water resources.

Interestingly, both of the urban volume metrics in 2000 and 2012 of the commercial area were highly correlated with the fragmentation of waterbody. In the commercial area, the water patch was mainly located between the CBD and the South Bank area. Human activities had greatly transformed the waters [83]. From 2000 to 2012, there were as many as six bridges across the Yarra River in the commercial area. The bridge divided the water patch and increased the fragmentation of the water patch. Many dining and shopping facilities stand at the two ends of the bridge. Compared with the area far away from the Yarra River, a more prosperous commercial and cultural system was formed, which increased VM and VSD in this area. In 2000, the angle between PD2 and VSD was the smallest, and the projection of PD2 on the VSD arrow was also the largest (Figure 10). This was probably because the construction of well-arranged buildings on both sides of the river highlighted the differences between the buildings and enhanced the scenery of the waterfront on both sides of the Yarra River. In addition, the urban volume metrics were highly correlated with the complexity of bare land in 2000 and the complexity of grassland in 2012, respectively. Although the form of the business area had long been established, there were still more or less undeveloped areas with a bare surface, it is convincing that

the less bare land, the greater the degree of development and land use intensity. Of course, the government also paid attention to protect the environment in the commercial area and more green spaces appeared, such as Batman Park, Queen Victoria Park, and Flagstaff Garden. However, the more fragmentation of grassland, the lower the VM and VSD. Considering the high cost of land resources in the commercial district, the development degree of grassland should be comprehensively adjusted in combination with the needs of economic development and environmental protection status.

In the future, Melbourne should continue to increase the development of both banks of the Yarra River, improve land use efficiency, enhance the landscape recognition and spatial differences, and build a more compact, prosperous, and functionally complex business center.

Our results demonstrated that the urban volume metrics of residential areas had changed from being highly correlated with the fragmentation of manmade coverage in 2000 to being highly correlated with the complexity of woodland, the fragmentation of grassland, and the fragmentation of bare land in 2012. In 2000, manmade coverage was dominated by concentrated and contiguous buildings and large-scale private houses which were mainly single-door, single-family two-story, resulting in highly connected patches. A larger LPI1 meant a larger VM and a higher level of urbanization. However, regular houses led to small VSD, which affected its spatial differences. After 2000, in response to Melbourne 2030, around the large and continuous woodland areas, such as Pridmore Park, Dickinson Reserve, and O'Connell Reserve, hospital (Australian Physiotherapy Council), gymnasium (Fitness First Richmond Victoria Gardens), department store (Victoria Gardens Shopping Centre) and other public service centers were sporadically built by the government. These buildings, as an important part of public facilities, were in sharp contrast with the surrounding low-rise residential buildings and bare land, such as construction sites, which appeared inevitably during this period, leading to the increasing of VM and VSD. Far away from protected areas and parks, private residences were still dominated. Richmond, one of the most environmentally friendly districts in Melbourne, had always thought highly of protecting the green space. The increase of green space such as street trees could reduce the heat island effect of residential areas and control the microclimate [43,84], provided a comfortable and pleasant sensory experience [85,86], and improved the health and well-being of residents [87,88]. The low-density residential distribution, interspersed with green spaces between the residential houses, resulted in low VM and VSD compared with public facilities.

In the future, urban planners should take Richmond as the template to develop new residential areas. The government should build forest land around the residential areas in advance to adjust the climate and purify the air. Based on taking into account the accessibility of service facilities and the accessibility of public services, the activity center and supporting facilities (such as hospitals, gymnasiums, shopping malls, etc.) should be planned according to the structure of the resident group and the density of residence [89]. The vertical differences between public facilities and private residences should be enhanced to form a landmark and recognizable city intention. Furthermore, attention should also be paid to the construction of the internal environment, increasing the area of street trees and grass in a limited space, and enhancing the overall greenness of the residential area.

These suggestions above were based on objective and rigorous data analysis and could provide different planning strategies for each functional area.

5. Conclusions

Exploring the relationship between the 2D landscape pattern and 3D urban volume is of great significance for understanding the social and ecological effects of cities, especially in compact cities. With the support of RS and GIS, our study used Melbourne as the research area to study spatial and temporal changes of land use and urban volume since the 21st century, found out the key landscape metrics that had a high correlation with the urban

volume from different scales and clarified the interaction mechanism between landscape pattern and urban volume. Finally, we gave corresponding development suggestions.

From 2000 to 2012, the manmade coverage, woodland, and grassland of Melbourne had changed a lot. Patches became regular and reunited, with a trend of decreasing fragmentation and complexity, increasing connectivity. The bare land had decreased sharply, and the waterbody had been generally stable. Urbanization and vertical differentiation had increased. In terms of vertical dimensions, both VM and VSD presented a “high–low” situation from the city center to the surroundings, maintaining the distribution of “large east and small west”. In the entire study area, patches with low fragmentation and high aggregation were directly proportional to high VM with high value. In addition, patches with high connectivity and fragmentation had a positive relationship with high VSD. The urban volume metrics of different urban functional areas were affected by different landscape factors, and their internal mechanisms were revealed in light of the actual development situation, which was affected by many aspects, such as environmental characteristics, economic development level, and policy implementation. The research results would be a big step forward for observing and understanding the linkage between landscape patterns and urban volume in compact cities. Furthermore, when the urban volume is hard to calculate, we can accurately and scientifically express the urban development characteristics by employing the landscape metrics through the results of this study. In the future, we will focus on the comparative study of the relationship between the landscape pattern and urban volume of different cities, because cities with different development models (horizontal expansion such as Bern, Lausanne, and Zurich in Swiss [18], vertical expansion such as Melbourne) may have different results. In addition, we plan to adopt remote sensing images and elevation data sets with higher resolution, higher precision, and larger range for more refined research.

Author Contributions: Conceptualization, Mengyu Ge, Shenghui Fang and Wenbing Gong; methodology, Mengyu Ge and Yan Gong; resources, Mengyu Ge and Pengjie Tao; writing—original draft Preparation, Mengyu Ge; writing—review and editing, Mengyu Ge, Guang Yang and Yan Gong; supervision, Yan Gong; project administration, Shenghui Fang. All authors have read and agreed to the published version of the manuscript.

Funding: This research received no external funding.

Data Availability Statement: The data presented in this study are available on request from the corresponding author.

Acknowledgments: We thank the editors and the anonymous reviewers for their valuable comments and suggestions.

Conflicts of Interest: The authors declare no conflict of interest.

Appendix A

Table A1. Regression equations between landscape metrics and VM.

VM								
Year	Landscape Metrics	Regression Equations	R ²	Pearson	Landscape Metrics	Regression Equations	R ²	Pearson
2000	PD	$Y = 132.32x^{0.83}$	0.27 **	+	PLAND3	NSc		
2012		$Y = 861.39x^{0.54}$	0.17 **	-		NSc		
2000	LPI	$Y = -0.38x^2 + 81.64x - 756.29$	0.13 **	+	PD3	$Y = -2.80x^2 + 157.47x + 1708.60$	0.15 **	+
2012		$Y = -0.42x^2 + 115.23x - 1594.9$	0.17 **	+		NSc		
2000	LSI	NSc			LPI3	NSc		
2012		$Y = -471.94x^2 + 2178.3x + 2823.9$	0.12 **	-		NSc		
2000	AI	NSc			LSI3	$Y = 1012.40e^{0.24x}$	0.14 **	+
2012		$Y = -13.11x^2 + 2407.3x - 105175$	0.11 **	+		$Y = -233.24x^2 + 1536.1x + 2961.2$	0.12 **	+
2000	CONTAG	$Y = 2.38x^{1.72}$	0.30 **	+	AI3	$Y = -1.53x^2 + 134.06x + 553.31$	0.18 **	+
2012		$Y = 0.73x^{2.05}$	0.48 **	+		$Y = -1.36x^2 + 121.8x + 2835.2$	0.16 **	+
2000	COHESION	NSc			COHESION3	$Y = -0.98x^2 + 108.05x + 580.20$	0.17 **	+
2012		$Y = -109.35x^2 + 21490x - 1E + 6$	0.11 **	+		$Y = -1.21x^2 + 124.18x + 2543.6$	0.22 **	+
2000	SHDI	$Y = 3651.6x^{0.77}$	0.25 **	-	PLAND4	NSc		
2012		$Y = -2563.1x^2 + 1714.6x + 5239.3$	0.16 **	-		$Y = 1.83x^2 - 154.93x + 5589.2$	0.13 **	-
2000	PLAND1	$Y = 15.60x^{1.22}$	0.88 **	+	PD4	NSc		
2012		$Y = 45.46x^{1.06}$	0.92 **	+		$Y = -27x^2 + 180.77x + 4975.9$	0.11 **	-
2000	PD1	NSc			LPI4	NSc		
2012		NSc				$Y = 8.29x^2 - 285.33x + 5602.2$	0.11 **	-
2000	LPI1	$Y = 22.67x^{1.15}$	0.85 **	+	LSI4	NSc		
2012		$Y = 54.43x^{1.03}$	0.91 **	+		$Y = -383.91x^2 + 1336.8x + 4272.4$	0.11 **	-
2000	LSI1	$Y = 778.89x^{1.20}$	0.27 **	-	AI4	NSc		
2012		$Y = 2509.3x^{0.73}$	0.15 **	-		$Y = -1.29x^2 + 116.14x + 3092$	0.13 **	-
2000	AI1	$Y = 4E - 05x^{3.99}$	0.81 **	+	COHESION4	$Y = -0.94x^2 + 91.21x + 1404.10$	0.15 **	+
2012		$Y = 0.01x^{3.3}$	0.82 **	+		$Y = -1.46x^2 + 121.31x + 3439.5$	0.25 **	-
2000	COHESION1	$Y = 0.48e^{0.09x}$	0.87 **	+	PLAND5	$Y = -78.08x + 3634.90$	0.15 **	-
2012		$Y = 3.89e^{0.07x}$	0.88 **	+		NSc		
2000	PLAND2	$Y = 3204.6e^{-0.04x}$	0.57 **	-				
2012		$Y = 5231.1e^{-0.04x}$	0.65 **	-				

Table A1. Cont.

VM								
Year	Landscape Metrics	Regression Equations	R ²	Pearson	Landscape Metrics	Regression Equations	R ²	Pearson
2000	PD2	$Y = 233.24x^2 - 983.41x + 3199.5$	0.24 **	+	PD5	NSc		
2012		$Y = 90.96x^2 - 569.15x + 5047.5$	0.26 **	+		NSc		-
2000	LPI2	$Y = 3183.8e^{-0.05x}$	0.58 **	-	LPI5	$Y = 5.69x^2 - 229.21x + 3660.40$	0.14 **	-
2012		$Y = 5276.4e^{-0.04x}$	0.66 **	-		NSc		
2000	LSI2	NSc			LSI5	$Y = -64.89x^2 + 79.70x + 3672.90$	0.11 **	-
2012		$Y = 994.12x^2 - 2472.1x + 5301.8$	0.21 **	+		NSc		-
2000	AI2	$Y = 3245.20e^{-0.01x}$	0.16 **	-	AI5	$Y = -33.26x + 4561$	0.14 **	-
2012		$Y = -0.78 + 44.11x + 5149.8$	0.23 **	-		NSc		
2000	COHESION2	$Y = 3209.70e^{-0.01x}$	0.15 **	-	COHESION5	$Y = -0.24x^2 - 4.27x + 4093.10$	0.18 **	-
2012		$Y = -0.88x^2 + 55.08x + 5098.9$	0.23 **	-		NSc		

** Correlation is significant at the 0.01 level (2-tailed). + means positive correlation. - means negative correlation. (Note: PLAND = Percentage of Landscape, PD = Patch Density, LPI = Largest Patch Index, LSI = Landscape Shape Index, AI = Aggregation Index, CONTAG = Contagion Index, COHESION = Patch Cohesion Index, SHDI = Shannon's Diversity Index. VM = volume mean, VSD = Volume Standard Deviation. 1 = Manmade coverage, 2 = Waterbody, 3 = Woodland, 4 = Grassland, 5 = Bare land).

Table A2. Regression equations between landscape metrics and VSD.

VSD								
Year	Landscape Metrics	Regression Equations	R ²	Pearson	Landscape Metrics	Regression Equations	R ²	Pearson
2000	PD	$Y = 226.46x^{0.65}$	0.39 **	+	PLAND3	$Y = -3.39x^2 + 156.34x + 1795.70$	0.20 **	+
2012		$Y = 815.41x^{0.48}$	0.33 **	+		NSc		
2000	LPI	NSc			PD3	$Y = -3.92x^2 + 193.73x + 1025.40$	0.30 **	+
2012		NSc				NSc		
2000	LSI	$Y = 876.3x^{0.85}$	0.22 **	+	LPI3	NSc		
2012		$Y = 2123.4x^{0.59}$	0.16 **	+		NSc		
2000	AI	$Y = 44223e^{-0.03x}$	0.13 **	-	LSI3	$Y = 947.05e^{0.24x}$	0.31 **	+
2012		NSc				$Y = 2310.8e^{0.14x}$	0.15 **	+
2000	CONTAG	NSc			AI3	$Y = 1124.30e^{0.02x}$	0.16 **	+
2012		$Y = 171.28x^{0.71}$	0.14 **	+		$Y = 2171e^{0.01x}$	0.16 **	+
2000	COHESION	$Y = 2E + 08^{-0.12x}$	0.13 **	-	COHESION3	$Y = 1035.30e^{0.01x}$	0.23 **	+
2012		NSc				$Y = 2178.2e^{0.01x}$	0.18 **	+

Table A2. Cont.

VSD								
Year	Landscape Metrics	Regression Equations	R ²	Pearson	Landscape Metrics	Regression Equations	R ²	Pearson
2000	SHDI	$Y = 3240.20x^{0.71}$	0.51 **	+				
2012		$Y = 4881.8x^{0.38}$	0.29 **	+				
2000	PLAND1	$Y = 158.09x^{0.64}$	0.57 **	+	PLAND4	NSc		
2012		$Y = 353.46x^{0.53}$	0.55 **	+		NSc		
2000	PD1	$Y = 1412.6x^{0.42}$	0.22 **	+	PD4	NSc		
2012		$Y = 2693.2x^{0.29}$	0.15 **	+		NSc		
2000	LPI1	$Y = 213.85x^{0.58}$	0.50 **	+	LPI4	NSc		
2012		$Y = 409.44x^{0.50}$	0.51 **	+		NSc		
2000	LSI1	$Y = 850.94x^{1.01}$	0.46 **	+	LSI4	NSc		
2012		$Y = 1951.8x^{0.77}$	0.39 **	+		NSc		
2000	AI1	$Y = 0.08x^{2.29}$	0.62 **	+	AI4	$Y = 1141.80e^{0.01x}$	0.13 **	+
2012		$Y = 1141.80e^{0.01x}$	0.55 **	+		NSc		
2000	COHESION1	$Y = 0.23x^{2.02}$	0.70 **	+	COHESION4	$Y = 1216.30e^{0.01x}$	0.13 **	+
2012		$Y = 1.84x^{1.65}$	0.63 **	+		NSc		
2000	PLAND2	$Y = 2579.3e^{-0.02x}$	0.38 **	-	PLAND5	NSc		
2012		$Y = 3803.9e^{-0.02x}$	0.37 **	-		NSc		
2000	PD2	$Y = 101.86x^2 - 109.67x + 2347.6$	0.29 **	+	PD5	NSc		
2012		$Y = 23.08x^2 + 217.17x + 3378.2$	0.37 **	+		NSc		
2000	LPI2	$Y = 2574.9e^{-0.02x}$	0.40 **	-	LPI5	NSc		
2012		$Y = 3796.2e^{-0.02x}$	0.40 **	-		NSc		
2000	LSI2	$Y = 472.28x + 2264$	0.11 **	+	LSI5	NSc		
2012		$Y = 451.5x^2 - 382.88x + 3450.6$	0.28 **	+		NSc		
2000	AI2	$Y = -0.68x^2 + 60.88x + 2262$	0.16 **	+	AI5	NSc		
2012		$Y = -0.91x^2 + 79.4x + 3393.6$	0.20 **	+		NSc		
2000	COHESION2	$Y = -0.71x^2 + 64.36x + 2260.70$	0.16 **	+	COHESION5	NSc		
2012		$Y = -0.97x^2 + 86.17x + 3384.7$	0.21 **	+		NSc		

** Correlation is significant at the 0.01 level (2-tailed). + means positive correlation. - means negative correlation. (Note: PLAND = Percentage of Landscape, PD = Patch Density, LPI = Largest Patch Index, LSI = Landscape Shape Index, AI = Aggregation Index, CONTAG = Contagion Index, COHESION = Patch Cohesion Index, SHDI = Shannon's Diversity Index. VM = volume mean, VSD = Volume Standard Deviation. 1 = Manmade coverage, 2 = Waterbody, 3 = Woodland, 4 = Grassland, 5 = Bare land).

Table A3. SLR parameters of VM, VSD and class-level landscape metrics in industrial area.

2000							2012						
VM				VSD			VM				VSD		
Landscape Metrics	Standardized Coefficients	Tolerance	VIF	Standardized Coefficients	Tolerance	VIF	Landscape Metrics	Standardized Coefficients	Tolerance	VIF	Standardized Coefficients	Tolerance	VIF
LPI3	−0.390 **	0.477	2.098	–	–	–	COHESION2	–	–	–	0.573 **	0.685	1.460
AI3	0.156 **	0.517	1.936	–	–	–	PLAND3	−0.454 **	0.464	2.157	–	–	–
COHESION3	–	–	–	0.281 **	0.854	1.171	PD3	0.281 **	0.333	3.000	–	–	–
PD4	–	–	–	−0.303 **	0.476	2.100	PD4	0.325 **	0.624	1.603	−0.447 **	0.685	1.460
LPI4	–	–	–	0.324 **	0.669	1.494	R ²		0.22			0.82	
COHESION4	−0.113 **	0.411	2.433	–	–	–							
PD5	0.688 **	0.555	1.800	−0.366 **	0.554	1.805							
LPI5	−0.206 **	0.279	3.582	–	–	–							
AI5	–	–	–	−0.247 **	0.736	1.359							
COHESION5	0.251 **	0.308	3.244	–	–	–							
R ²		0.81			0.53								

– means this variable is discarded. ** Correlation is significant at the 0.01 level. (Note: PLAND = Percentage of Landscape, PD = Patch Density, LPI = Largest Patch Index, LSI = Landscape Shape Index, AI = Aggregation Index, CONTAG = Contagion Index, COHESION = Patch Cohesion Index, SHDI = Shannon's Diversity Index. VM = volume mean, VSD = Volume Standard Deviation. 1 = Manmade coverage, 2 = Waterbody, 3 = Woodland, 4 = Grassland, 5 = Bare land).

Table A4. SLR parameters of VM, VSD and class-level landscape metrics in commercial area.

2000							2012						
VM				VSD			VM				VSD		
Landscape Metrics	Standardized Coefficients	Tolerance	VIF	Standardized Coefficients	Tolerance	VIF	Landscape Metrics	Standardized Coefficients	Tolerance	VIF	Standardized Coefficients	Tolerance	VIF
PD2	–	–	–	0.611 **	0.769	1.301	PD2	–	–	–	0.491 **	0.866	1.155
COHESION2	–	–	–	0.090 **	0.578	1.730	AI3	−0.319 **	0.664	1.506	−0.135 **	0.628	1.593
PD4	–	–	–	−0.226 **	0.634	1.577	LSI4	−0.441 **	0.604	1.657	−0.278 **	0.705	1.419
AI4	−0.437 **	1.000	1.000	–	–	–	LSI5	−0.554 **	0.565	1.770	–	–	–
LSI5	–	–	–	−0.163 **	0.632	1.583	AI5	0.248 **	0.530	1.888	–	–	–
AI5	–	–	–	−0.054 **	0.805	1.242	R ²		0.61			0.47	
R ²		0.19			0.59								

– means this variable is discarded. ** Correlation is significant at the 0.01 level. (Note: PLAND = Percentage of Landscape, PD = Patch Density, LPI = Largest Patch Index, LSI = Landscape Shape Index, AI = Aggregation Index, CONTAG = Contagion Index, COHESION = Patch Cohesion Index, SHDI = Shannon's Diversity Index. VM = volume mean, VSD = Volume Standard Deviation. 1 = Manmade coverage, 2 = Waterbody, 3 = Woodland, 4 = Grassland, 5 = Bare land).

Table A5. SLR parameters of VM, VSD and class-level landscape metrics in residential area.

2000							2012						
VM			VSD				VM			VSD			
Landscape Metrics	Standardized Coefficients	Tolerance	VIF	Standardized Coefficients	Tolerance	VIF	Landscape Metrics	Standardized Coefficients	Tolerance	VIF	Standardized Coefficients	Tolerance	VIF
PD1	–	–	–	0.429 **	0.550	1.818	LSI3	−0.347 **	0.646	1.548	–	–	–
LPI1	0.842 **	0.185	5.416	–	–	–	COHESION3	–	–	–	0.541 **	0.811	1.233
PD3	–	–	–	0.157 **	0.680	1.470	PLAND4	–	–	–	−0.077 **	0.990	1.010
COHESION3	0.194 **	0.337	2.965	–	–	–	AI4	−0.170 **	0.746	1.340	–	–	–
PLADN4	−0.331 **	0.210	4.769	–	–	–	LPI5	–	–	–	0.530 **	0.818	1.222
AI4	−0.094 **	0.633	1.579	–	–	–	LSI5	0.214 **	0.642	1.557	–	–	–
COHESION4	–	–	–	0.190 **	0.695	1.438	R ²		0.08			0.83	
LSI5	0.218 **	0.475	2.104	0.226 **	0.547	1.829							
R ²		0.80			0.63								

– means this variable is discarded. ** Correlation is significant at the 0.01 level. (Note: PLAND = Percentage of Landscape, PD = Patch Density, LPI = Largest Patch Index, LSI = Landscape Shape Index, AI = Aggregation Index, CONTAG = Contagion Index, COHESION = Patch Cohesion Index, SHDI = Shannon's Diversity Index. VM = volume mean, VSD = Volume Standard Deviation. 1 = Manmade coverage, 2 = Waterbody, 3 = Woodland, 4 = Grassland, 5 = Bare land).

References

1. Bian, Z.; Wang, S.; Wang, Q.; Yu, M.; Qian, F. Effects of urban sprawl on arthropod communities in peri-urban farmed landscape in Shenbei New District, Shenyang, Liaoning Province, China. *Sci. Rep.* **2018**, *8*, 101. [\[CrossRef\]](#)
2. Schneider, A.; Mertes, C.M. Expansion and growth in Chinese cities, 1978–2010. *Environ. Res. Lett.* **2014**, *9*, 024008. [\[CrossRef\]](#)
3. Li, X.; Liu, X.; Gong, P. Integrating ensemble-urban cellular automata model with an uncertainty map to improve the performance of a single model. *Int. J. Geogr. Inf. Sci.* **2015**, *29*, 762–785. [\[CrossRef\]](#)
4. Effat, H.A.; El Shobaky, M.A. Modeling and Mapping of Urban Sprawl Pattern in Cairo Using Multi-Temporal Landsat Images, and Shannon's Entropy. *Adv. Remote Sens.* **2015**, *04*, 303–318. [\[CrossRef\]](#)
5. Peng, Y.; Wang, Q.; Wang, H.; Lin, Y.; Song, J.; Cui, T.; Fan, M. Does landscape pattern influence the intensity of drought and flood? *Ecol. Indic.* **2019**, *103*, 173–181. [\[CrossRef\]](#)
6. Seto, K.C.; Guneralp, B.; Hutya, L.R. Global forecasts of urban expansion to 2030 and direct impacts on biodiversity and carbon pools. *Proc. Natl. Acad. Sci. USA* **2012**, *109*, 16083–16088. [\[CrossRef\]](#) [\[PubMed\]](#)
7. Peng, J.; Ma, J.; Liu, Q.; Liu, Y.; Hu, Y.; Li, Y.; Yue, Y. Spatial-temporal change of land surface temperature across 285 cities in China: An urban-rural contrast perspective. *Sci. Total Environ.* **2018**, *635*, 487–497. [\[CrossRef\]](#)
8. Hua, S.; Jing, H.; Yao, Y.; Guo, Z.; Lerner, D.N.; Andrews, C.B.; Zheng, C. Can groundwater be protected from the pressure of China's urban growth? *Environ. Int.* **2020**, *143*, 105911. [\[CrossRef\]](#)
9. Yang, G.; Zhao, Y.; Xing, H.; Fu, Y.; Liu, G.; Kang, X.; Mai, X. Understanding the changes in spatial fairness of urban greenery using time-series remote sensing images: A case study of Guangdong-Hong Kong-Macao Greater Bay. *Sci. Total Environ.* **2020**, *715*, 136763. [\[CrossRef\]](#)
10. Shi, L.; Wurm, M.; Huang, X.; Zhong, T.; Leichtle, T.; Taubenböck, H. Urbanization that hides in the dark-Spotting China's "ghost neighborhoods" from space. *Landsc. Urban Plan.* **2020**, *200*, 103822. [\[CrossRef\]](#)
11. Rimal, B.; Zhang, L.; Keshtkar, H.; Wang, N.; Lin, Y. Monitoring and Modeling of Spatiotemporal Urban Expansion and Land-Use/Land-Cover Change Using Integrated Markov Chain Cellular Automata Model. *ISPRS Int. J. Geo-Inf.* **2017**, *6*, 288. [\[CrossRef\]](#)
12. Peng, J.; Liu, Y.; Wu, J.; Lv, H.; Hu, X. Linking ecosystem services and landscape patterns to assess urban ecosystem health: A case study in Shenzhen City, China. *Landsc. Urban Plan.* **2015**, *143*, 56–68. [\[CrossRef\]](#)
13. Wu, J.; Hobbs, R. Key issues and research priorities in landscape ecology: An idiosyncratic synthesis. *Landsc. Ecol.* **2002**, *17*, 355–365. [\[CrossRef\]](#)
14. Li, X.; Yeh, A.G. Analyzing spatial restructuring of land use patterns in a fast growing region using remote sensing and GIS. *Landsc. Urban Plan.* **2004**, *69*, 335–354. [\[CrossRef\]](#)
15. Yu, X.; Ng, C. An integrated evaluation of landscape change using remote sensing and landscape metrics: A case study of Panyu, Guangzhou. *Int. J. Remote Sens.* **2006**, *27*, 1075–1092. [\[CrossRef\]](#)
16. Weng, Q. Land use change analysis in the Zhujiang Delta of China using satellite remote sensing, GIS and stochastic modelling. *J. Environ. Manag.* **2002**, *64*, 273–284. [\[CrossRef\]](#)
17. Ji, W.; Ma, J.; Twibell, R.W.; Underhill, K. Characterizing urban sprawl using multi-stage remote sensing images and landscape metrics. *Comput. Environ. Urban Syst.* **2006**, *30*, 861–879. [\[CrossRef\]](#)
18. Bosch, M.; Jaligot, R.; Chenal, J. Spatiotemporal patterns of urbanization in three Swiss urban agglomerations: Insights from landscape metrics, growth modes and fractal analysis. *Landsc. Ecol.* **2020**, *35*, 879–891. [\[CrossRef\]](#)
19. Qiu, J.; Wang, X.; Lu, F.; Ouyang, Z.; Zheng, H. The spatial pattern of landscape fragmentation and its relations with urbanization and socio-economic developments: A case study of Beijing. *Acta Ecol. Sin.* **2012**, *32*, 2659–2669.
20. Felt, C.; Fragkias, M.; Larson, D.; Liao, H.; Lohse, K.A.; Lybecker, D. A comparative study of urban fragmentation patterns in small and mid-sized cities of Idaho. *Urban Ecosyst.* **2018**, *21*, 805–816. [\[CrossRef\]](#)
21. Silva, P.; Li, L. Mapping Urban Expansion and Exploring Its Driving Forces in the City of Praia, Cape Verde, from 1969 to 2015. *Sustainability* **2017**, *9*, 1434. [\[CrossRef\]](#)
22. Qin, J.; Fang, C.; Wang, Y.; Li, G.; Wang, S. Evaluation of three-dimensional urban expansion: A case study of Yangzhou City, Jiangsu Province, China. *Chin. Geogr. Sci.* **2015**, *25*, 224–236. [\[CrossRef\]](#)
23. He, S.; Wang, X.; Dong, J.; Wei, B.; Duan, H.; Jiao, J.; Xie, Y. Three-Dimensional Urban Expansion Analysis of Valley-Type Cities: A Case Study of Chengguan District, Lanzhou, China. *Sustainability* **2019**, *11*, 5663. [\[CrossRef\]](#)
24. Zheng, Z.; Zhou, W.; Wang, J.; Hu, X.; Qian, Y. Sixty-Year Changes in Residential Landscapes in Beijing: A Perspective from Both the Horizontal (2D) and Vertical (3D) Dimensions. *Remote Sens.* **2017**, *9*, 992. [\[CrossRef\]](#)
25. Shi, L.; Foody, G.M.; Boyd, D.S.; Girindran, R.; Wang, L.; Du, Y.; Ling, F. Night-time lights are more strongly related to urban building volume than to urban area. *Remote Sens. Lett.* **2019**, *11*, 29–36. [\[CrossRef\]](#)
26. Qiao, W.; Liu, Y.; Wang, Y.; Lu, Y. Analysis on the characteristics of three-dimensional urban space expansion in Nanjing since 2000. *Geogr. Res.* **2015**, *34*, 666–676.
27. van Leeuwen, C.J. Water governance and the quality of water services in the city of Melbourne. *Urban Water J.* **2017**, *14*, 247–254. [\[CrossRef\]](#)

28. Sokolov, S.; Black, K.P. Modelling the time evolution of water-quality parameters in a river: Yarra River, Australia. *J. Hydrol.* **1996**, *178*, 311–335. [\[CrossRef\]](#)
29. Coutts, A.M.; Beringer, J.; Tapper, N.J. Impact of Increasing Urban Density on Local Climate: Spatial and Temporal Variations in the Surface Energy Balance in Melbourne, Australia. *J. Appl. Meteorol. Clim.* **2007**, *46*, 477–493. [\[CrossRef\]](#)
30. Department of Sustainability and Environment. *Melbourne 2030: Planning for Sustainable Growth*, State of Victoria; Department of Sustainability and Environment: Melbourne, Australia, 2002; p. 192.
31. Zhang, H.; Wang, T.; Zhang, Y.; Dai, Y.; Jia, J.; Yu, C.; Li, G.; Lin, Y.; Lin, H.; Cao, Y. Quantifying Short-Term Urban Land Cover Change with Time Series Landsat Data: A Comparison of Four Different Cities. *Sensors* **2018**, *18*, 4319. [\[CrossRef\]](#)
32. Feranec, J.; Jaffrain, G.; Soukup, T.; Hazeu, G. Determining changes and flows in European landscapes 1990–2000 using CORINE land cover data. *Appl. Geogr.* **2010**, *30*, 19–35. [\[CrossRef\]](#)
33. Gong, P.; Wang, J.; Yu, L.; Zhao, Y.; Zhao, Y.; Liang, L.; Niu, Z.; Huang, X.; Fu, H.; Liu, S.; et al. Finer resolution observation and monitoring of global land cover: First mapping results with Landsat TM and ETM+ data. *Int. J. Remote Sens.* **2012**, *34*, 2607–2654. [\[CrossRef\]](#)
34. Xiao, R.; Huang, X.; Yu, W.; Lin, M.; Zhang, Z. Interaction Relationship between Built-Up Land Expansion and Demographic-Social-Economic Urbanization in Shanghai-Hangzhou Bay Metropolitan Region of Eastern China. *Photogramm. Eng. Remote Sens.* **2019**, *85*, 231–240. [\[CrossRef\]](#)
35. Li, X.; Gong, P.; Liang, L. A 30-year (1984–2013) record of annual urban dynamics of Beijing City derived from Landsat data. *Remote Sens. Environ.* **2015**, *166*, 78–90. [\[CrossRef\]](#)
36. Gong, W.; Fang, S.; Yang, G.; Ge, M. Using a Hidden Markov Model for Improving the Spatial-Temporal Consistency of Time Series Land Cover Classification. *ISPRS Int. J. Geo-Inf.* **2017**, *6*, 292. [\[CrossRef\]](#)
37. Hulshoff, R.M. Landscape indices describing a Dutch landscape. *Landsc. Ecol.* **1995**, *10*, 101–111. [\[CrossRef\]](#)
38. Peng, J.; Wang, Y.; Zhang, Y.; Wu, J.; Li, W.; Li, Y. Evaluating the effectiveness of landscape metrics in quantifying spatial patterns. *Ecol. Indic.* **2010**, *10*, 217–223. [\[CrossRef\]](#)
39. Griffiths, G.H.; Lee, J. Landscape pattern and species richness; regional scale analysis from remote sensing. *Int. J. Remote Sens.* **2000**, *21*, 2685–2704. [\[CrossRef\]](#)
40. Junxiang, L.; Yujie, W.; Xiaohong, S.; Yongchang, S. Landscape pattern analysis along an urban-rural gradient in the Shanghai metropolitan region. *Acta Ecol. Sin.* **2004**, *24*, 1973–1980.
41. Saura, S. Effects of remote sensor spatial resolution and data aggregation on selected fragmentation indices. *Landsc. Ecol.* **2004**, *19*, 197–209. [\[CrossRef\]](#)
42. Wu, Q.; Guo, F.; Li, H.; Kang, J. Measuring landscape pattern in three dimensional space. *Landsc. Urban Plan.* **2017**, *167*, 49–59. [\[CrossRef\]](#)
43. Zhou, W.; Cao, F.; Wang, G. Effects of Spatial Pattern of Forest Vegetation on Urban Cooling in a Compact Megacity. *Forests* **2019**, *10*, 282. [\[CrossRef\]](#)
44. He, H.S.; DeZonia, B.E.; Mladenoff, D.J. An aggregation index (AI) to quantify spatial patterns of landscapes. *Landsc. Ecol.* **2000**, *15*, 591–601. [\[CrossRef\]](#)
45. Chuncheng, Z.; Youshui, Z.; Huanhuan, H. Impacts of Impervious Surface Area and Landscape Metrics on Urban Heat Environment in Fuzhou City, China. *J. Geo-Inf. Sci.* **2014**, *16*, 490–498.
46. Hagen-Zanker, A. A computational framework for generalized moving windows and its application to landscape pattern analysis. *Int. J. Appl. Earth Obs.* **2016**, *44*, 205–216. [\[CrossRef\]](#)
47. Park, Y.; Guldman, J. Measuring continuous landscape patterns with Gray-Level Co-Occurrence Matrix (GLCM) indices: An alternative to patch metrics? *Ecol. Indic.* **2020**, *109*, 105802. [\[CrossRef\]](#)
48. Chen, Y.; Li, X.; Liu, X.; Ai, B. Modeling urban land-use dynamics in a fast developing city using the modified logistic cellular automaton with a patch-based simulation strategy. *Int. J. Geogr. Inf. Sci.* **2014**, *28*, 234–255. [\[CrossRef\]](#)
49. Fan, C.; Myint, S. A comparison of spatial autocorrelation indices and landscape metrics in measuring urban landscape fragmentation. *Landsc. Urban Plan.* **2014**, *121*, 117–128. [\[CrossRef\]](#)
50. Yang, Q.; Li, J.; Gan, X.; Zhang, J.; Yang, F.; Qian, Y. Comparison of landscape patterns between metropolises and small-sized cities: A gradient analysis with changing grain size in Shanghai and Zhangjiagang, China. *Int. J. Remote Sens.* **2012**, *33*, 1446–1464. [\[CrossRef\]](#)
51. Luck, M.; Wu, J. A gradient analysis of urban landscape pattern: A case study from the Phoenix metropolitan region, Arizona, USA. *Landsc. Ecol.* **2002**, *17*, 327–339. [\[CrossRef\]](#)
52. Zhang, J.; Li, S.; Dong, R.; Jiang, C. Physical evolution of the Three Gorges Reservoir using advanced SVM on Landsat images and SRTM DEM data. *Environ. Sci. Pollut. Res.* **2018**, *25*, 14911–14918. [\[CrossRef\]](#) [\[PubMed\]](#)
53. Priestnall, G.; Jaafar, J.; Duncan, A. Extracting urban features from LiDAR digital surface models. *Comput. Environ. Urban Syst.* **2000**, *24*, 65–78. [\[CrossRef\]](#)
54. Ali, Z.; Nasir, S.; Iqbal, I.A.; Shahzad, A. Accuracy Assessment of Digital Elevation Model Generated from Pleiades Tri stereo-pair. In Proceedings of the International Conference on Recent Advances in Space Technologies, Istanbul, Turkey, 16–19 June 2015.
55. Yao, X.; Sun, M.; Gong, P.; Liu, B.; Li, X.; An, L.; Yan, L. Overflow probability of the Salt Lake in Hoh Xil Region. *J. Geogr. Sci.* **2018**, *28*, 647–655. [\[CrossRef\]](#)

56. Islam, M.A.; Thenkabail, P.S.; Kulawardhana, R.W.; Alankara, R.; Gunasinghe, S.; Edussriya, C.; Gunawardana, A. Semi-automated methods for mapping wetlands using Landsat ETM+ and SRTM data. *Int. J. Remote Sens.* **2008**, *29*, 7077–7106. [\[CrossRef\]](#)
57. Wu, Q.; Song, C.; Liu, K.; Ke, L. Integration of TanDEM-X and SRTM DEMs and Spectral Imagery to Improve the Large-Scale Detection of Opencast Mining Areas. *Remote Sens.* **2020**, *12*, 1451. [\[CrossRef\]](#)
58. Zhang, Q.; Yang, Q.; Cheng, J.; Wang, C. Characteristics of 3" SRTM Errors in China. *Geomat. Inf. Sci. Wuhan Univ.* **2018**, *43*, 684–690.
59. Nelson, A.D.; Reuter, H.I.; Gessler, P.; Hengl, T.; Reuter, H.I. Dem Production methods and sources. *Dev. Soil Sci.* **2009**, *33*, 65–85.
60. Kelldorfer, J.; Walker, W.; Pierce, L.; Dobson, C.; Fites, J.A.; Hunsaker, C.; Vona, J.; Clutter, M. Vegetation height estimation from Shuttle Radar Topography Mission and National Elevation Datasets. *Remote Sens. Environ.* **2004**, *93*, 339–358. [\[CrossRef\]](#)
61. Guo, J.; Kong, X. *Foundation of Geodesy*; Wuhan University Press: Wuhan, China, 2005.
62. Kwon, J.H.; Bae, T.; Choi, Y.; Lee, D.; Lee, Y. Geodetic datum transformation to the global geocentric datum for seas and islands around Korea. *Geosci. J.* **2005**, *9*, 353–361. [\[CrossRef\]](#)
63. Li, Y.C.; Sideris, M.G.; Schwarz, K. A numerical investigation on height anomaly prediction in mountainous areas. *Bull. Géodésique* **1995**, *69*, 143–156. [\[CrossRef\]](#)
64. Zhang, F.; Wang, J.; Luo, H. The Comparative and Analysis of Seven-parameter Coordinate Conversion Model. *Geomat. Spat. Inf. Technol.* **2016**, *39*, 48–51.
65. Fu, F.; Liu, Z.; Huang, Q. Three-dimensional urban landscape pattern changes: A case study in the Central Business District of Futian, Shenzhen. *Acta Ecol. Sin.* **2019**, *39*, 4299–4308.
66. Zhao, Y.; Ovando-Montejo, G.A.; Frazier, A.E.; Mathews, A.J.; Flynn, K.C.; Ellis, E.A. Estimating work and home population using lidar-derived building volumes. *Int. J. Remote Sens.* **2017**, *38*, 1180–1196. [\[CrossRef\]](#)
67. Liu, M.; Hu, Y.; Li, C. Landscape metrics for three-dimensional urban building pattern recognition. *Appl. Geogr.* **2017**, *87*, 66–72. [\[CrossRef\]](#)
68. Qu, B.; Ling, J.; Ma, J. A study on the quantitative description and evaluation method of street spatial form in the city business district. *New Archit.* **2019**, *06*, 9–14.
69. Yang, J.; Shi, Y. Approaches and Methods of Urban Vertical Control in Overall Urban Design. *Urban Plan. Forum.* **2015**, *06*, 90–98.
70. Yang, J. *Urban Central District Planning Theories and Methods*; Southeast University Press: Nanjing, China, 2013.
71. Li, Z.; You, H.; Wang, Z. Multi-scale effects of urban landscape pattern on plant diversity in Xuzhou City, Jiangsu Province, China. *Chin. J. Appl. Ecol.* **2018**, *29*, 1813–1821.
72. Jingwei, H.; Yiyang, Z.; Chengming, T.; Dianguang, X.; Yingmei, L. Effects of Regional Landscape Pattern on the Epidemic of Poplar Rust Disease: A Case Study of Populus alba in Yanqing, Beijing. *Sci. Silvae Sin.* **2020**, *56*, 99–108.
73. Duan, M.; Liu, Y.; Yu, Z.; Li, L.; Wang, C.; Axmacher, J.C. Environmental factors acting at multiple scales determine assemblages of insects and plants in agricultural mountain landscapes of northern China. *Agric. Ecosyst. Environ.* **2016**, *224*, 86–94. [\[CrossRef\]](#)
74. Song, Y.; Song, X.; Shao, G.; Hu, T. Effects of Land Use on Stream Water Quality in the Rapidly Urbanized Areas: A Multiscale Analysis. *Water-Sui.* **2020**, *12*, 1123. [\[CrossRef\]](#)
75. Djoudi, E.A.; Plantegenest, M.; Aviron, S.; Pétilion, J. Local vs. landscape characteristics differentially shape emerging and circulating assemblages of carabid beetles in agroecosystems. *Agric. Ecosyst. Environ.* **2019**, *270–271*, 149–158. [\[CrossRef\]](#)
76. Zhang, J.; Li, S.; Jiang, C. Effects of land use on water quality in a River Basin (Daning) of the Three Gorges Reservoir Area, China: Watershed versus riparian zone. *Ecol. Indic.* **2020**, *113*, 106226. [\[CrossRef\]](#)
77. Stevens, Q.; Hao, C.; Zhang, S.; Xu, C.; Tie, J. The Design of Urban Waterfronts—A Critique of Two Australian “Southbanks” (Sequel). *J. Qingdao Technol. Univ.* **2008**, *77*, 173–203.
78. Ye, M. *Cases and Studies on the Suburban Development Policies of Developed Countries*; China Architecture & Building Press: Beijing, China, 2010.
79. Wu, W.; Zhao, S.; Zhu, C.; Jiang, J. A comparative study of urban expansion in Beijing, Tianjin and Shijiazhuang over the past three decades. *Landsc. Urban Plan.* **2015**, *134*, 93–106. [\[CrossRef\]](#)
80. Li, G.; Sun, S.; Fang, C. The varying driving forces of urban expansion in China: Insights from a spatial-temporal analysis. *Landsc. Urban Plan.* **2018**, *174*, 63–77. [\[CrossRef\]](#)
81. Chien, S. Local farmland loss and preservation in China: A perspective of quota territorialization. *Land Use Policy* **2015**, *49*, 65–74. [\[CrossRef\]](#)
82. Shukla, A.; Jain, K. Critical analysis of spatial-temporal morphological characteristic of urban landscape. *Arab. J. Geosci.* **2019**, *12*, 112. [\[CrossRef\]](#)
83. Anim, A.K.; Thompson, K.; Duodu, G.O.; Tschärke, B.; Birch, G.; Goonetilleke, A.; Ayoko, G.A.; Mueller, J.F. Pharmaceuticals, personal care products, food additive and pesticides in surface waters from three Australian east coast estuaries (Sydney, Yarra and Brisbane). *Mar. Pollut. Bull.* **2020**, *153*, 111014. [\[CrossRef\]](#)
84. Bonan, G.B. The microclimates of a suburban Colorado (USA) landscape and implications for planning and design. *Landsc. Urban Plan.* **2000**, *49*, 97–114. [\[CrossRef\]](#)
85. Mehta, V. Walkable streets: Pedestrian behavior, perceptions and attitudes. *J. Urban. Int. Res. Placemaking Urban Sustain.* **2008**, *1*, 217–245. [\[CrossRef\]](#)

-
86. de Bell, S.; White, M.; Griffiths, A.; Darlow, A.; Taylor, T.; Wheeler, B.; Lovell, R. Spending time in the garden is positively associated with health and wellbeing: Results from a national survey in England. *Landsc. Urban Plan.* **2020**, *200*, 103836. [[CrossRef](#)]
 87. Marshall, A.J.; Grose, M.J.; Williams, N.S.G. From little things: More than a third of public green space is road verge. *Urban For. Urban Green.* **2019**, *44*, 126423. [[CrossRef](#)]
 88. Bratman, G.N.; Hamilton, J.P.; Daily, G.C. The impacts of nature experience on human cognitive function and mental health. *Ann. N. Y. Acad. Sci.* **2012**, *1249*, 118–136. [[CrossRef](#)] [[PubMed](#)]
 89. Coutts, A.M.; Beringer, J.; Tapper, N.J. Investigating the climatic impact of urban planning strategies through the use of regional climate modelling: A case study for Melbourne, Australia. *Int. J. Clim.* **2008**, *28*, 1943–1957. [[CrossRef](#)]